

Expression of an interleukin-2 partial agonist enhances regulatory T cell persistence and efficacy in mouse autoimmune models

Received: 20 June 2024

Accepted: 14 May 2025

Published online: 27 May 2025

 Check for updates

Janie Robert¹, Manon Feuillolay^{1,2}, María de Temple-Llavero¹, Reginald Florian Akossi¹, Vanessa Mhanna^{1,2}, Mustapha Cheraï², Gwladys Fourcade¹, Frédéric Charlotte³, Nicolas Tchitchek¹, Tian Mi⁴, Benjamin Youngblood⁴, Thomas Vazquez⁵, Michelle Rosenzweig^{1,2} & David Klatzmann^{1,2}✉

Regulatory T (Treg)-based cell therapy holds promise for autoimmune and inflammatory diseases, yet challenges remain regarding the functional stability and persistence of transferred Tregs. Here we engineer Tregs to express a partial agonist form of IL-2 (IL-2pa) to enhance persistence while avoiding toxicity from excessive signaling. Mouse Tregs expressing wild-type IL-2 (Tregs-IL2wt) have only a transient growth advantage, limited by toxicity from likely excessive signaling. By contrast, mouse Tregs-IL2pa exhibit sustained expansion, long-term survival in immunocompetent mice for over a year, and bystander expansion of endogenous Tregs. Tregs-IL2pa maintain a stable activated phenotype, Treg-specific demethylation, and a diverse TCR repertoire. In vivo, prophylactic transfer of Tregs-IL2pa ameliorates multi-organ autoimmunity in a Treg depletion-induced mouse autoimmune model. Lastly, compared with control Treg, human Tregs-IL2pa show enhanced survival in the IL-2-depleted environment of immune-deficient mice and improved control of xenogeneic graft-versus-host disease. Our results thus show that IL-2pa self-sufficiency enhances the stability, durability and efficacy of Treg therapies in preclinical settings.

The pivotal role of CD4⁺CD25⁺Foxp3⁺ regulatory T cells (Tregs) in controlling autoimmune and inflammatory diseases¹ has made them a prime target for therapeutic intervention. Low-dose IL-2 (IL-2_{LD}) and IL-2 muteins are in advanced clinical development as Treg stimulators, with some promising indications of efficacy^{2–4}. However, the in vivo broad stimulation of endogenous Tregs might not be sufficient in some clinical settings such as those with high inflammation. In such settings, Treg-based cell therapies have emerged as a potential solution. They involve the isolation of Tregs generally from the patient's

blood, followed by ex vivo cell expansion and subsequent infusion back into the patient. These therapies are currently under clinical investigation for hematopoietic stem cell transplantation, graft-versus-host disease (GVHD), solid organ transplantation, and various autoimmune diseases⁵. The feasibility and safety of these therapies have been substantiated. Currently, over 25 phase I/II clinical trials evaluating Treg-based therapy across various diseases are in progress, but only a few phase II results have been released, with no definitive proof of efficacy reported^{6,7}. Nonetheless, early studies demonstrated

¹Sorbonne Université, INSERM, UMRS959, Immunology-Immunopathology-Immunotherapy (i3), F-75005 Paris, France. ²Assistance Publique - Hôpitaux de Paris, Clinical Investigation Center for Biotherapy and Immunology (CIC-BTi), Hôpital Pitié-Salpêtrière, F-75013 Paris, France. ³Assistance Publique - Hôpitaux de Paris, Pathology department, Hôpital Pitié-Salpêtrière, F-75013 Paris, France. ⁴Immunology, MS 351, St. Jude Children's Research Hospital, Memphis, USA.

⁵ILTOO Pharma, 10 rue des Reculettes, 75013 Paris, France. ✉e-mail: david.klatzmann@sorbonne-universite.fr

notable clinical improvements, such as symptom reduction in chronic GVHD and decreased insulin dependency in type 1 diabetes (T1D) patients post-Treg therapy^{8,9}. Treg cell therapies thus hold promises, notably because they can be engineered to incorporate additional properties such as being targeted or armored.

However, a critical limitation of Treg cell therapies lies in their limited survival within the host. A phase I clinical trial in T1D patients followed the adoptively transferred Tregs using deuterium labeling, and it revealed a rapid decline in the infused Treg numbers¹⁰. Deuterium levels peaked between days 7 to 14 and had decreased by over 75% at three months. This precipitous decline in infused Treg numbers post-injection could possibly result from a shortage of available interleukin-2 (IL-2) within the patients, as T1D patients have a genetically determined low IL-2 production^{11–13}.

Indeed, IL-2 is a cytokine essential for the survival, stability, and function of Tregs^{14,15}. Consequently, IL-2 is routinely supplemented in Treg cultures to support their expansion and maintain their regulatory phenotype. Treg culture necessitates one to five weeks of culture with the addition of substantial IL-2 levels, varying from 200 to 1000 International Units (IU)/mL throughout the culture period^{16–18}. After this IL-2 conditioning phase, in the presence of IL-2 concentration that can be over 3000-fold higher than IL-2 physiological serum concentration, Tregs might become “IL-2-addicted”, i.e., necessitate very high IL-2 to survive well. Likewise, they may suffer when injected in a patient who represents a low IL-2 concentration environment. One solution could be to supplement the recipient with IL-2 after the Treg infusion. However, the dose and duration of such treatment cannot be easily determined.

Since Tregs are inherently incapable of producing IL-2^{19–21}, we hypothesized that equipping Tregs with the ability to self-produce IL-2 could enhance their long-term viability. In addition, an IL-2-self-sufficiency should lead to their sustained activation. This in turn should increase their suppressive function, and consolidate the stability of their suppressive phenotype, likewise preventing them from converting to effector cells that they could do notably in high inflammatory environment^{22–25}.

In this work, we design, tune, and evaluate IL-2-self-sufficient Tregs (Tregs-IL2). We report that while expression of wild-type IL-2 leads to a rapid exhaustion of Tregs-IL2, the expression of IL-2 tuned to provide low biological activity could considerably improve Tregs-IL2 fitness, survival and prophylactic efficacy. Such Treg engineering has the potential to improve the effectiveness of any Treg-cell-based therapy.

Results

Adoptively transferred ex vivo cultured Tregs have a limited lifespan in mice

Since therapeutic Treg cell products necessitate the activation and expansion of Tregs in high IL-2 containing medium, we evaluated the survival of such cultured Tregs after their adoptive transfer in normal mice. Donor Tregs were purified from Thy1.1 mice, activated and expanded for 5 days. They were then transduced with a retroviral vector expressing the Thy1.2 reporter molecule and cultured for another 2 days, a time at which 9×10^5 non-sorted cultured Tregs (Ctrl Tregs) were adoptively transferred into B6 Thy1.2 mice (Fig. 1A, B). Ctrl Tregs had a CD25⁺Foxp3⁺ Treg phenotype, with > 42% of them being Thy1.2⁺ (Fig. 1A).

We monitored their fate in blood and tissues over an extended period. As exemplified in one representative experiment, we observed an initial increase in the proportion of blood Ctrl Tregs from day 7 to day 14 (Fig. 1C), a time at which they could be detected in tissues (Fig. 1D). Within these cells, in the blood, the proportion of transduced Thy1.2 cells and CD25⁺Foxp3⁺ cells remained stable (Supp. Fig. 1A, B). By day 26, there was a dramatic reduction in the percentage of Ctrl Tregs in the blood, exceeding a ten-fold decrease (Fig. 1C). Part of this

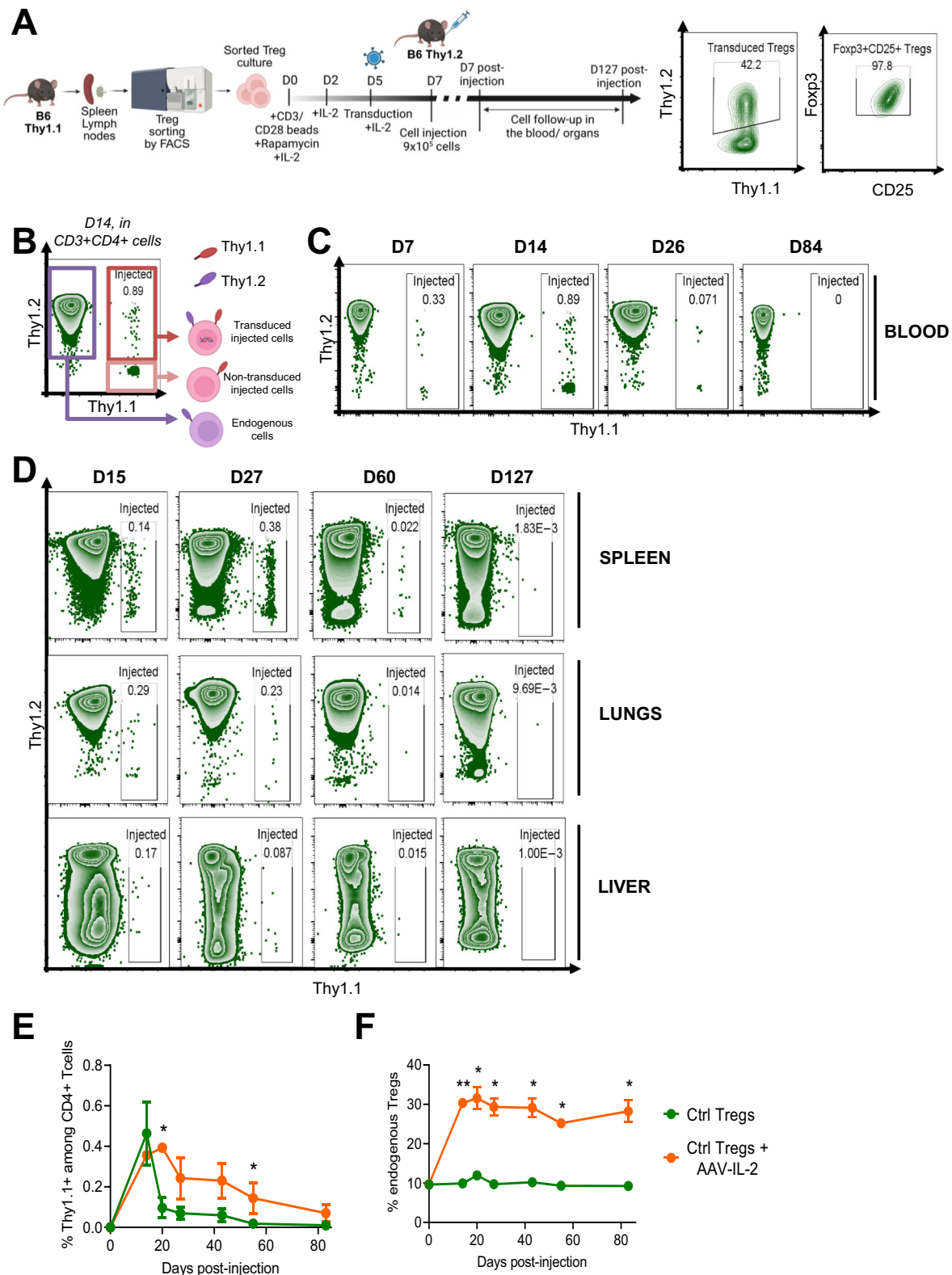
decrease could be due to a recirculation to the spleen in which the proportion of Tregs peaked at around day 26 (Fig. 1D). Nevertheless, in the blood, Ctrl Tregs were nearly undetectable by day 36, showing a significant decrease in their absolute number compared to day 14 (Supp. Fig. 1C), and had fully disappeared by day 84 (Fig. 1C). Similar results were obtained in four independent experiments (Fig. 1E, green line). In tissues, they were only but barely detectable in the spleen by day 60, and could no longer be detected in any tissue by day 127 (Fig. 1D).

These experiments highlight the limited survival of adoptively transferred cultured Tregs. We reasoned that this could be due to the Treg culture period in medium containing IL-2 at a concentration > 3000-fold higher than IL-2 plasmatic concentration²⁶. This could have rendered these Tregs “IL-2 addicted”, contributing to a poor survival when transferred in an environment with normal IL-2 concentration. We thus investigated whether continuous IL-2 production in mice could support Treg survival and prevent their rapid loss. To examine this hypothesis, we co-injected mice with Ctrl Tregs and an AAV-IL-2 enabling continuous production of wild-type IL-2. As indicated by the proportion of injected cells, AAV-IL-2 administration, significantly improved the early survival of Ctrl Tregs, resulting in a more than four-fold increase in the percentage of injected cells on day 20 compared to untreated mice (Fig. 1E). This significant enhancement in early cell survival was confirmed by the cell counts in the blood, with AAV-IL-2-treated mice showing a five-fold increase in Treg absolute number on day 20 (Supp. Fig. 1D). However, despite the continuous IL-2 production, Ctrl Tregs progressively declined and became nearly undetectable by day 83, similar to Ctrl Tregs in untreated mice. In contrast, endogenous Tregs in AAV-IL-2-treated mice expanded shortly after AAV injection and maintained a three-fold increase in their proportion among CD4⁺ T cells up to day 83 (Fig. 1F), highlighting the continuous IL-2 production.

IL-2-self-sufficient Treg survival in mice

We hypothesized that an autocrine production of IL-2 by Tregs would improve their survival. We transduced Thy1.1 Tregs with a retroviral vector encoding wild-type IL-2 and the Thy1.2 reporter gene (Tregs-IL2wt) or the reporter gene only (Ctrl Tregs). We injected 9×10^5 non-sorted cells into normal Thy1.2 recipient mice in which Thy1.1⁺Thy1.2⁺ transduced and Thy1.1⁺ untransduced donor Tregs could be tracked apart from Thy1.2⁺ endogenous Tregs (Fig. 1B). Consistent with earlier findings, Ctrl Tregs (green line) demonstrated poor survival in both blood and organs. In blood, Ctrl Tregs peaked on day 14, declined sharply by day 26, and were undetectable by 2 months (Fig. 2A). Surprisingly, Tregs-IL2wt (red line) exhibited a survival profile similar to that of Ctrl Tregs, in both blood and organs, despite their production of IL-2wt (Fig. 2A, B, H). However, we noticed that the percentage of Thy1.2⁺ transduced cells within the Tregs-IL2wt population (that also contained untransduced cells) had a sharp increase from about 40% on injection to 80% on day 14, and then decreased sharply to vanish on day 25 (Fig. 2C). This denotes an initial growth advantage of the IL-2wt transduced cells, followed by a marked growth disadvantage indicating toxicity. We reasoned that this could be due to an excessive tonic signaling by the permanent IL-2wt production. We thus aim to evaluate the fate of Tregs expressing IL-2 with a partial agonist activity (IL-2pa).

We tested a few such IL-2s and selected the one that provided the best survival in preliminary experiments (Supp. Fig. 2A). The selected IL-2pa featured a Stat-5 phosphorylation activity in Tregs that is 1,000 times lower than that of IL-2wt (Supp. Fig. 2B). Thy1.1 Tregs transduced with a retroviral vector encoding this IL-2pa and the Thy1.2 reporter gene (Tregs-IL2pa) had a completely different behavior than Tregs-IL2wt upon adoptive transfer. Tregs-IL2pa (blue line) showed a remarkable prolonged survival. On day 14, the percentage of Thy1.1⁺ Tregs-IL2pa represented about 5 % of the whole CD4 population, and was significantly higher than that of Ctrl Tregs (Fig. 2B). The survival of



Tregs-IL2pa remained stable between days 14 and 36, both in their proportion and absolute number in the blood (Fig. 2B, Supp. Fig. 2C, and D). Post day 36 of injection, Tregs-IL2pa percentages slowly rose to reach around 10% of CD4⁺ cells on day 126, which represents the usual percentage of endogenous Tregs in normal B6 mice. Noteworthy, the IL2pa transduced donor Tregs had a growth advantage compared to the untransduced donor cells, and already by day 25 their proportion

had doubled from 40 to over 80% (Fig. 2C). Tregs-IL2pa retained a CD25⁺Foxp3⁺ Treg phenotype (Fig. 2D).

The proportion and absolute number of endogenous Tregs remained stable at around 10% of the CD4⁺ cells in the blood of mice adoptively transferred with Tregs-IL2wt or Ctrl Tregs (Fig. 2E, Supp. Fig. 2E). In contrast, in Tregs-IL2pa mice, the percentage of endogenous Tregs had already doubled by day 14, and reached 65% of the CD4⁺

Fig. 1 | Adoptively transferred ex vivo cultured Tregs have a limited lifespan in mice. **A** Schematic experimental design. Created in BioRender⁴⁹. Tregs were isolated from the spleen and lymph nodes of male or female B6 Thy1.1 mice at six to twenty weeks of age. On day 5 of culture, the cells were transduced with the control vector MSCV-Thy1.2 for the expression of the reporter gene mouse Thy1.2 alone in the transduced cells. Two days post-transduction, 9×10^5 unsorted transduced control Tregs (Ctrl Tregs) per mouse were injected into B6 Thy1.2 mice aged six to twenty weeks. Recipient mice were sex-matched with the donor cells. Survival of the injected cells was tracked in the blood or organs of the mice, as indicated. Contour plots representing transduction efficacy and Treg purity on the day of cell injection are shown on the left. **B** Gating strategy for tracking Thy1.1 donor cells within the CD3⁺CD4⁺ population of Thy1.2 recipient mice. Transduced and non-transduced donor cells are Thy1.1⁺Thy1.2⁺ and Thy1.1⁺Thy1.2⁻, respectively; endogenous CD4 cells are Thy1.2⁺Thy1.1⁻. A zebra plot from the blood of a mouse

receiving Ctrl Tregs 14 days post-injection is shown. Schematic created in BioRender⁴⁹. **C** Dynamics of Thy1.1 donor Ctrl Tregs in the blood. Data were extracted from one representative out of four experiments with a total of $n = 8$. **D** Dynamics of Thy1.1 injected Ctrl Tregs in the spleen, lungs, and liver. **E, F** Dynamics of Ctrl Tregs (**E**) and endogenous Tregs (**F**) in the blood of recipient mice treated with an AAV-IL2 (orange, $n = 3$) or not (green, $n = 8$), from four independent experiments. Statistically significant differences were found between Ctrl Tregs injected into mice treated with AAV-IL2 and untreated mice on day 20 ($p = 0.0357$) and day 55 ($p = 0.0250$), and between endogenous Tregs in AAV-IL2-treated and untreated mice on days 14 ($p = 0.061$), 20 ($p = 0.0119$), 27 ($p = 0.0121$), 43 ($p = 0.0167$), 55 ($p = 0.0167$), and day 83 ($p = 0.0167$). Data are presented as mean \pm SEM in panels (**E**), and (**F**) and compared using a two-tailed Mann-Whitney test (* $p < 0.05$; ** $p < 0.01$; *** $p < 0.001$, **** $p < 0.0001$).

cells by day 126 in the blood. Tconv cells remained stable at 90% in mice receiving Tregs-IL2wt or Ctrl Tregs, but decreased in those that received Tregs-IL2pa inversely to the increase in proportion of the endogenous Tregs (Fig. 2F). Tconv absolute number in mice receiving Tregs-IL2pa were comparable to those in mice receiving Ctrl Tregs (Supp. Fig. 2F). There was no marked effect on NK cell proportion and absolute number (Fig. 2G, Supp. Fig. 2G). These observations on blood Tregs pertained to tissue Tregs. In the spleen, lungs, and liver, numbers of Tregs-IL2pa were much higher than those of Tregs-IL2wt (Fig. 2H), and there were also increased percentages of endogenous Tregs only in mice having received the Tregs-IL2pa (Fig. 2I).

The production of Treg cell products is a major hassle, and reducing the number of cells to be produced would be a significant improvement. Given the remarkable persistence and expansion of Tregs-IL2pa, we investigated the behavior of a nine-fold lower Tregs-IL2pa dose (Fig. 2J, K). Similar to the 9×10^5 cell dose, injected cells in the 1×10^5 cell dose continuously expanded, reaching a proportion of 4% of CD4 cells on day 126 (Fig. 2J). Endogenous CD4 Tregs were also enriched, proportionally to the increase of Tregs-IL2pa (Fig. 2K). Finally, the survival potential of Tregs-IL2pa was further tested by transplanting donor Tregs-IL2pa from a primary to a secondary recipient mouse. 250 μ l of whole blood from the primary recipient was transferred to secondary recipients. This sufficed to then detect a growing population of Tregs-IL2pa, and their accompanying increase of endogenous Tregs (Fig. 2L).

Given the high survival and expansion potential of Tregs-IL2pa, we aimed to test the safety potential of a kill-switch for conditional cell killing of Tregs-IL2pa. We used the presence of Thy1.1 onto these cells as a surrogate for the expression of classical kill-switches such as tEGR, RQR8 or CD20, which are currently used for ablating gene-modified cells in humans^{27–29}. Administering an anti-Thy1.1 antibody effectively depleted the Tregs-IL2pa cells (Fig. 2M). Seven days post-treatment, Thy1.1 cells could no longer be detected, and this depletion persisted for the entire follow-up (until day 190). This elimination of injected cells correlated with a progressive reduction in endogenous Tregs that had returned to their basal levels of around 13% by day 190.

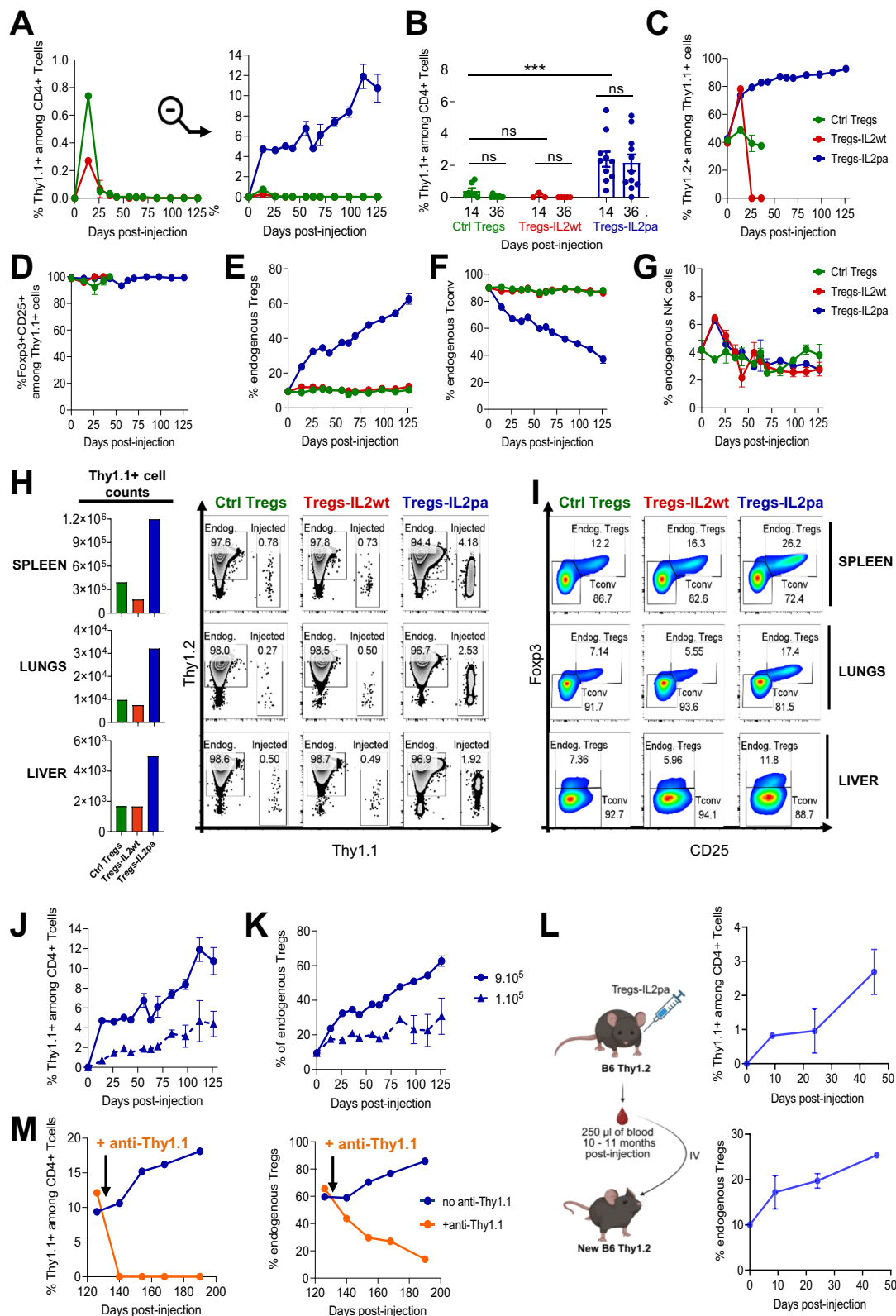
Altogether, in contrast to Tregs-IL2wt, Tregs-IL2pa have a remarkable growth advantage, produce an excess of IL-2pa that can rescue endogenous Tregs without any effects on effector T cells nor NK cells, and can be efficiently ablated on purpose.

Deep immunoprofiling of murine IL-2pa-self-sufficient Tregs

For a comprehensive characterization of Tregs-IL2pa, we analyzed their transcriptome profiles at the single-cell level. We sampled splenocytes six months after injection of Tregs-IL2pa, a time at which they constituted nearly 15% of CD4⁺ cells (Supp. Fig. 3A), from which we sorted Tregs-IL2pa and endogenous Tregs (Supp. Fig. 6A). We also purified “fresh” Tregs from an unmanipulated control mouse. The transcriptome profiles of these three Treg populations were analyzed jointly. The Uniform Manifold Approximation and Projection (UMAP)

representation revealed that each sample had distinct but closely related transcriptome profiles, highlighting both shared and unique characteristics (Fig. 3A). There was no overlap between the Ctrl Treg cell cluster and the cell clusters from the other two groups, which partially overlapped with each other. All three cell clusters similarly expressed Treg characteristic markers (Fig. 3B). Indeed, each cluster of cells appeared to be composed of two populations according to the levels of expression of Treg activation markers such as CD25, CTLA4, and GITR. Most Tregs were negative for markers of exhaustion/senescence such as KLRG1, LAG3 and TIGT (Fig. 3C). A small subpopulation of endogenous Tregs had a high expression of these three markers, together with a high expression of Treg activation markers (Fig. 3B). In comparison to the transcriptome of IL-2pa-stimulated endogenous Tregs, Tregs-IL2pa displayed differential gene expression primarily associated with protein translation and metabolism (Supp. Fig. 3B). The expression of Treg activation/functional markers was further confirmed at the protein level through flow cytometry analysis (Fig. 3D, Supp. Fig. 3C). These results extended and refined the transcriptomic studies revealing that Tregs-IL2pa maintained the expression of key activation markers, with several markers such as GITR and CD39 showing higher expression on Tregs-IL2pa and endogenous Tregs compared to fresh Tregs. Almost all Tregs-IL2pa and endogenous Tregs expressed Helios, indicating their thymic origin³⁰. Noteworthy, Tregs-IL2pa expressed the highest levels of ICOS, a molecule that controls Treg survival by tuning the expression of multiple anti-apoptotic genes³¹.

Tregs rely on IL-2 and TCR stimulation for survival and proliferation^{32–34}. The robust proliferation and long-term survival of Tregs-IL2pa indicate that they receive sustained TCR-mediated stimulation. To delve deeper into the clonality of these cells, we performed bulk TCR β sequencing of the same three Treg populations, the Ctrl Tregs being further separated into naïve and activated/memory-Tregs (nTregs and amTregs, respectively) based on CD44 and CD62L expression³⁵. From the 500,000 sorted Tregs-IL2pa, we identified 3000 unique clonotypes, indicating a polyclonal repertoire. The Renyi's entropy curve, which evaluates the repertoire clonality through a continuum of measures defined by an α parameter, revealed that the IL-2pa-expanded endogenous Tregs have a comparable repertoire diversity to that of fresh amTregs (Fig. 3E). Their diversity falls between the nTregs, which show a higher diversity, and the Tregs-IL2pa being the least diverse repertoire among all the populations. The Renyi values for $\alpha > 4$ were the lowest for Tregs-IL2pa, indicating the presence of expansions. These results clearly indicate that each of these four repertoires is polyclonal, with increasing expansions from fresh nTregs to fresh amTregs to endogenous Tregs and then to Tregs-IL2pa. These expansions are further evidenced by analyzing the proportion of clonotypes within the overall repertoire according to their count (Fig. 3F). In fresh nTregs, most clonotypes are represented less than 100 times, while in fresh amTregs and endogenous Tregs, a large fraction of clonotypes are represented up to 10,000 times. Expansions



are further pronounced in Tregs-IL2pa with more clonotypes being represented more than 10,000 times.

To complete the characterization of Tregs-IL2pa, we analyzed their methylation profile for the Tregs Specific Demethylation Region (TSDR) to ensure that continuous IL-2 production does not affect the stability of Foxp3 expression at the epigenetic level. Similar to fresh Tregs, sorted Tregs-IL2pa exhibited complete demethylation of TSDR,

confirming stable Foxp3 expression (Fig. 3G). Notably, TSDR in endogenous Tregs was also completely demethylated.

Finally, we assessed the phenotype of the cells after injection into RAG immunodeficient mice. These mice lack mature T cell, thereby drastically limiting endogenous IL-2 availability. When injected into RAG mice, Ctrl Tregs exhibited a rapid partial loss of their CD25⁺Foxp3⁺ Treg phenotype, with only 40% of the cells retaining the CD25⁺Foxp3⁺

Fig. 2 | IL-2-self-sufficient Treg survival in mice. **A** Dynamics of injected cells in the blood. Six- to twenty-week-old B6 Thy1.2 mice received 9×10^5 transduced unsorted Ctrl Tregs (green line), Tregs-IL2wt (red line) or Tregs-IL2pa (blue line) in a representative experiment, $n = 2$ per group. **B** Proportion of injected cells among CD3⁺CD4⁺ cells on days 14 and 36 post-injection in four independent experiments with Ctrl Tregs ($n = 8$), Tregs-IL2wt ($n = 5$) and Tregs-IL2pa ($n = 11$). Statistically significant difference was found between Ctrl Tregs and Tregs-IL2pa on day 14 ($p = 0.007$). **C** Proportion of transduced cells monitored as Thy1.2⁺ among Thy1.1⁺ in injected cells ($n = 2$). **D** Treg phenotype analysis of CD25⁺Foxp3⁺ expression among injected cells ($n = 2$). **E** Endogenous CD4 Tregs, **F** endogenous CD4 conventional T cells (Tconv), **G** natural killer (NK) cells among the endogenous cells, tracked in the blood ($n = 2$). **H** Injected cell counts and zebra plots from spleen, lungs, and liver

stained 14 days post-injection. **I** Pseudocolor plots of endogenous CD4 Tregs and Tconv from spleen, lungs, and liver 14 days post-injection. **J** Dynamics of injected Tregs and **K** endogenous CD4 Tregs in mice receiving either 9×10^5 or 1×10^5 Tregs-IL2pa, $n = 2$ per group. **L** Blood transfers from a primary Tregs-IL2pa recipient mouse to secondary unmanipulated recipient mice ($n = 3$), each receiving 250 μ L of blood collected 10–11 months post-injection. Injected Tregs (top panel) and endogenous Tregs (bottom panel) were tracked in the blood of the recipient mice. Schematic created in BioRender⁴⁹. **M** Depletion of injected cells using an anti-Thy1.1 antibody. Data are presented as mean \pm SEM in the panels (**A–G**) and (**J–L**). Data are compared using a two-tailed Mann-Whitney test in panel B ($^*p < 0.05$; $^{**}p < 0.01$; $^{***}p < 0.001$, $^{****}p < 0.0001$).

phenotype from day 14 to day 36 (Fig. 3H). In contrast, Tregs-IL2pa maintained a stable Treg phenotype, with 98% of the cells remaining CD25⁺Foxp3⁺ up to day 36. Furthermore, the entire population of injected Tregs-IL2pa exhibited higher expression of CD25 and Foxp3 compared to Ctrl Tregs, as indicated by the MFIs (Supp. Fig. 3D).

Murine IL-2pa-self-sufficient Tregs are suppressive in vitro and in vivo

We evaluated the Tregs-IL2pa suppressive capacity in a classical in vitro suppression assay using cultured cells harvested three days post-transduction. Decreasing proportions of Tregs were added to CTV-stained CD3/CD28 stimulated Tconv. Sorted transduced Ctrl Tregs and Tregs-IL2pa exhibited comparable suppressive activities in vitro (Fig. 4A, Supp. Fig. 6B). These results also indicate that the IL-2pa secreted by Tregs-IL2pa do not cause bystander activation of Tconv cells.

To assess the suppressive function of Tregs-IL2pa in vivo, we analyzed their capacity to control the catastrophic multi-organ autoimmunity caused by Treg depletion³⁶. We reasoned that this model will not only assess the in vivo suppressive function of Tregs-IL2pa, but also demonstrate the broadness of this suppression for multiple autoantigens. We used B6 Foxp3^{DTTR} - Thy1.2 mice as recipients of Tregs-IL2pa. Twenty days after the adoptive cell transfer, a time at which endogenous and Tregs-IL2pa represented 20 and 2.5% of CD4 cells, respectively, we treated mice with diphtheria toxin (DT) (Fig. 4B). Three days later, endogenous Tregs had been eliminated and stayed very low for another week (Fig. 4C). This endogenous Treg ablation triggered a delayed rise in Tregs-IL2pa that peaked at 18% of CD4 cells on day 10 (Fig. 4D). Weight loss (Fig. 4E) and accompanying clinical manifestations such as diarrhea (Fig. 4F) were considerable after endogenous Treg ablation in control mice that had lost 20% of their body weight on day 20, the time at which they were euthanized (Fig. 4E, F). They had a spleen size that was 10-fold higher than control mice (Fig. 4G), and they showed major signs of tissue inflammation in the colon, the lungs, and the liver (Fig. 4H, I). In contrast, mice with Tregs-IL2pa had a moderate weight loss of around 5%, no clinical signs, and almost no increase in spleen size except for one mouse. They also had very little tissue inflammation (Fig. 4H, I). Noteworthy, within the Tregs-IL2pa group, one mouse had a partial disease control, with some degree of splenomegaly and liver inflammation (Fig. 4H, Supp. Fig. 4A); this mouse had the lowest number of Tregs-IL2pa that peaked at 7.5% of CD4 cells on day 10 compared to 17.5% to 25% in the other mice (Supp. Fig. 4B). Altogether, this experiment demonstrates that Tregs-IL2pa efficiently control catastrophic multiorgan autoimmunity.

Human Tregs-IL2pa characterization in vitro

We generated human Tregs-IL2pa by lentiviral vectors mediated transduction of purified CD4⁺CD25⁺CD127^{low} blood Tregs. We first assessed their proliferation properties in vitro (Fig. 5A). Tregs-IL2pa and control Tregs expressing only the GFP reporter gene (Ctrl Tregs) similarly proliferated when activated and cultured in the presence of exogenous IL-2 (Fig. 5B), while only the Tregs-IL2pa proliferated in the

absence of exogenous IL-2 (Fig. 5C). Of note, when no stimulation and no exogenous IL-2 were used, neither the control nor the Tregs-IL2pa proliferated (Fig. 5D), indicating the strong dependency of Treg proliferation on both TCR and IL-2R signaling.

We next compared the transcriptome of purified Tregs-IL2pa to that of cultured Tregs transduced only with a reporter gene (Supp. Fig. 6C), as well as to that of freshly isolated Tregs. Multidimensional Scaling (MDS) representation generated based on the whole transcriptome expression showed that the cultured and transduced cells had similar transcriptome profiles, distinct from freshly isolated Tregs (Fig. 5E). When restricted to the transcriptome of the cultured cells only, the MDS revealed some modest but consistent changes that positioned cells from the three different donors closer to each other for each condition. Differential gene expression analysis of Foxp3, CD25, ICOS, and TNFRSF4 revealed higher expression levels in cells exposed to exogenous or autocrine IL-2 compared to cultures entirely deprived of IL-2 (Fig. 5F). Furthermore, in comparison to the transcriptome of transduced Ctrl Tregs, the transcriptomes of transduced Tregs-IL2pa exhibited differentially expressed genes primarily related to the IL-2 signaling and glycolysis pathways (Fig. 5G, H).

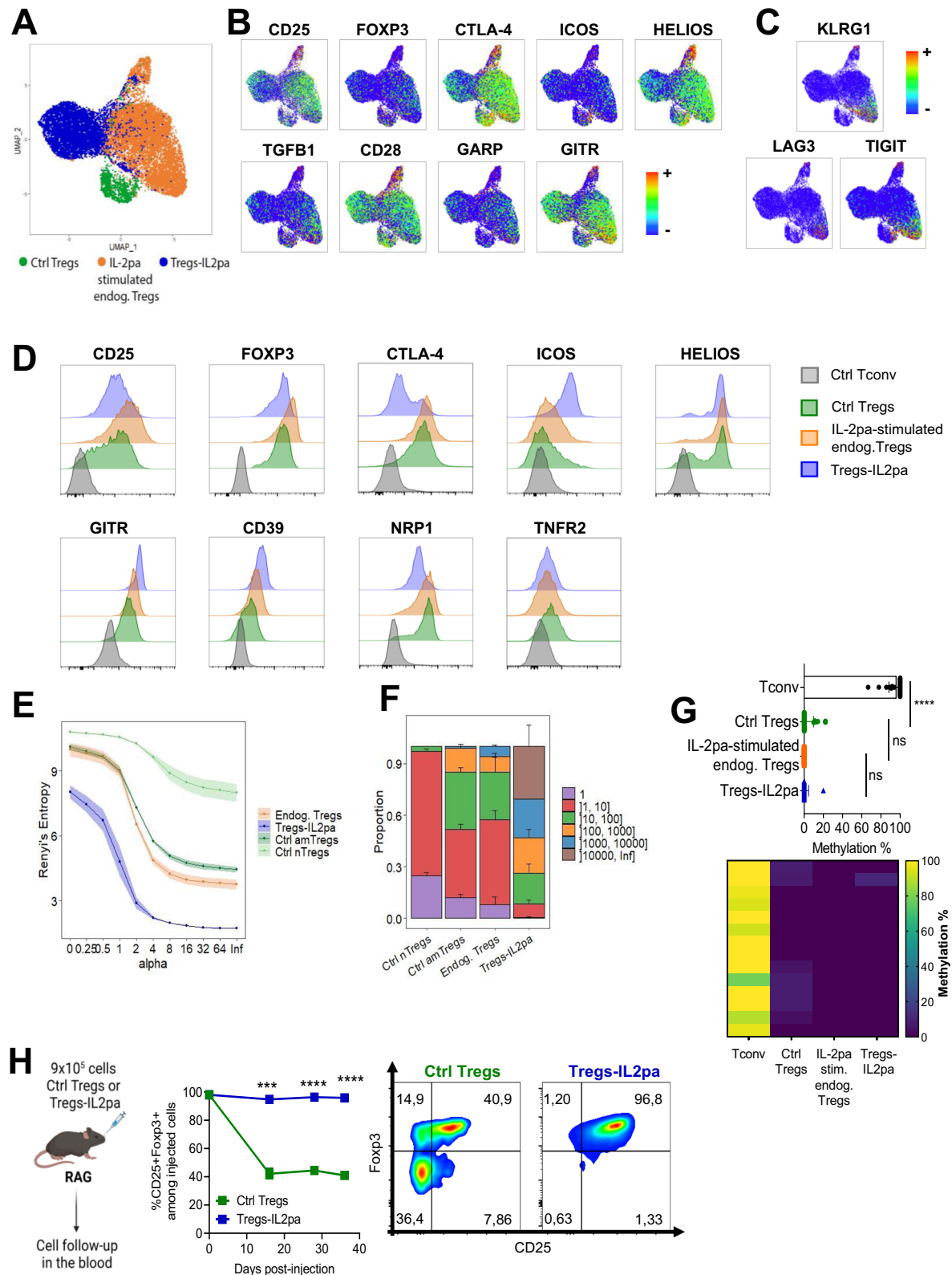
We evaluated the suppressive activity of human Tregs-IL2pa. As observed for murine Tregs-IL2pa, human Ctrl Tregs and Tregs-IL2pa exhibited similar suppression (Fig. 5I). These results further indicate that the possible excess IL-2pa produced by Tregs-IL2pa does not have any bystander effect on Tconv.

Human Tregs-IL2pa have long-term survival and improved suppressive function in immunodeficient recipient mice

We evaluated human Tregs-IL2pa survival in NSG mice that lack T cells, NK cells, B cells, thereby removing most IL-2 sources. We injected non-sorted Ctrl Tregs and Tregs-IL2pa into NSG mice and first monitored their survival in the blood. Up to day 21 post-injection, Ctrl Tregs and Tregs-IL2pa displayed similar survival profiles (Fig. 6A). Thereafter, Ctrl Tregs started to decrease while Tregs-IL2pa underwent significant expansion. On day 36, there were over 150-fold more Tregs-IL2pa than Ctrl Tregs in the blood.

On day 49, we analysed Tregs-IL2pa and Ctrl Tregs survival in the spleen, lungs, and liver. As in the blood, there were >100-fold more Tregs-IL2pa than Ctrl Tregs in tissues (Fig. 6B). The few surviving Ctrl Tregs retained CD25 and Foxp3 expression, albeit at lower levels than in Tregs-IL2pa in the liver (Fig. 6C, Supp. Fig. 5A). Tregs-IL2pa also exhibited elevated expressions of phenotypic and functional markers such as ICOS, CD39, and CTLA4 (Supp. Fig. 5B).

Finally, to evaluate Tregs-IL2pa's in vivo suppressive capabilities, we used the xenogeneic GVHD model obtained by injecting CD25-depleted PBMCs to NSG mice either alone or alongside with Tregs. To optimize the chances to highlight a functional difference between Ctrl Tregs and Tregs-IL2pa, we used a stringent model in which the Treg to Teff ratio was of 1 to 2. This setup revealed that mice receiving only PBMCs suffered from severe xenogeneic GVHD within 4–5 weeks, as shown by significant weight loss and high



mortality rates (Fig. 6D). As expected, at a 1/2 Tregs/Teff ratio, Ctrl Tregs failed to halt disease progression, with these mice experiencing weight loss and death similar to the PBMC-only group. In contrast, Tregs-IL2pa could control the disease, with limited weight loss and a 65% survival rate. These findings indicate the superior suppressive activity of human Tregs-IL2pa in highly inflammatory environments.

Discussion

Treg cell therapy has shown promising outcomes in treating autoimmune diseases and other inflammatory conditions^{5,8,9}. There are 3 major issues with the development of Treg cell therapy products, which have not been encountered for Teff cell products. These are their production, their survival, and their stability³⁷. First, Tregs have a complex and expensive process of production, which typically

Fig. 3 | Deep immunoprofiling of murine IL-2pa-self-sufficient Tregs. **A** UMAP representation of single-cell transcriptome profiles of sorted Treg samples obtained from splenocytes of a 32-week-old B6 Thy1.2 mouse that received Tregs-IL2pa. Splenocyte samples include purified IL-2pa-stimulated endogenous Tregs (orange) and transduced Tregs-IL2pa (blue). Tregs from an unmanipulated B6 Foxp3-GFP control mouse (Ctrl Tregs, green) were used as controls. **B** Colored UMAP representation based on the expression of selected Treg activation/function markers, scaled from lowest gene expression in blue to highest in red. **C** UMAP representation of KLRG1, LAG3, and TIGIT senescence/exhaustion markers. **D** Representative expression profiles of Treg activation and functional markers from blood flow cytometry staining. Ctrl Tregs and Ctrl Tconv were obtained from unmanipulated mice ($n = 3$), and IL-2pa-stimulated endogenous Tregs and Tregs-IL2pa were obtained from mice receiving Tregs-IL2pa ($n = 3$). Stainings were performed 5 to 7 months post-injection. **E** TCR diversity Renyi profiles for each condition ($n = 2$ per group). Colored circles represent the mean across samples within the same group and shaded areas represent the standard deviation (SD). **F** Barplot representation of the proportion of each defined clone count interval within the

total repertoire for each condition ($n = 2$ per group). Error bars indicate the standard error (SE). **G** Methylation analysis of the Treg Specific Demethylated Region (TSDR) with the average percentage of methylation for 14 CpG sites at the top and data for each CpG residue at the bottom, in Tconv ($n = 2$), IL-2pa-stimulated endogenous Tregs ($n = 2$) and Tregs-IL2pa ($n = 2$), and in Ctrl Tregs ($n = 3$). Statistically significant difference was found between Tconv and Ctrl Tregs ($p < 0.0001$). **H** Treg phenotype of injected cells after their transfer into RAG immunodeficient mice. Six- to seven-week-old male RAG mice received 9×10^5 transduced unsorted Ctrl Tregs or Tregs-IL2pa with $n = 3$ per group. Cell phenotype was monitored in the blood. The percentage of CD25⁺Foxp3⁺ cells among the injected cells is shown on the left, while a pseudocolor plot representing CD25⁺Foxp3⁺ staining 36 days post-injection is shown on the right. Schematic created in BioRender⁴⁹. Statistically significant differences were observed between Tregs-IL2pa and Ctrl Tregs on days 16 ($p = 0.0002$), 28, and 36 ($p < 0.0001$). Data are presented as mean \pm SEM in the panels (**G**, **H**) and compared using a two-tailed Mann-Whitney test in panel (**G**) and a two-tailed unpaired t-test in panel (**H**) (* $p < 0.05$; ** $p < 0.01$; *** $p < 0.001$, **** $p < 0.0001$).

involves cell sorting, two weeks of expansion, and often genetic modifications that altogether represent a significant hurdle. Second and even more critical, the short-lived persistence of injected cells could be a major limitation of Treg cell therapy. For instance, autologous non-modified expanded Tregs in T1D patients showed a decline 14 days post-injection and became scarcely detectable in circulation within three months¹⁰. This limited longevity was similarly observed in our study, where cultured murine Tregs adoptively transferred in immunocompetent mice progressively disappeared starting 14 days post-injection. This short survival is due in part to an insufficient IL-2 availability as supplementing recipient mice with endogenous IL-2 though an AAV-IL2 injection increased survival, although in a time-limited manner. Third, Tregs can be unstable, converting to an effector phenotype in high inflammatory settings^{22–25}. We hypothesized that making Tregs IL-2-self-sufficient could circumvent each of these 3 hurdles.

This was not the case when expressing the IL-2wt, which appeared toxic with time. However, IL-2wt-self-sufficient Tregs had an initial growth advantage as the percentage of IL-2wt expressing cells within the adoptively transferred Tregs rose from 40 to 80%. Hypothesizing that this could be due to an excessive tonic signaling by IL-2wt, this led us to investigate whether IL-2s with partial agonist properties could overcome this limitation. We indeed could find an IL-2pa with a 1000-fold reduced capacity for stat5 phosphorylation that demonstrated exceptional capacity to sustain long-term survival of IL-2-self-sufficient Tregs. These cells survived beyond one year in immunocompetent mice, not only in the bloodstream but also in organs like the spleen, lungs, and liver. Moreover, they could even be transferred from a primary recipient to a secondary recipient, in which they expanded. Tregs-IL2pa also retained their survival benefits and their capacity to activate endogenous Tregs when administered at a 9-fold lower dose, underscoring the likely reduced need for manufacturing large quantities of these cells. These observations demonstrate that the survival issue of Treg cell therapy products is fully solved by the expression of IL-2pa.

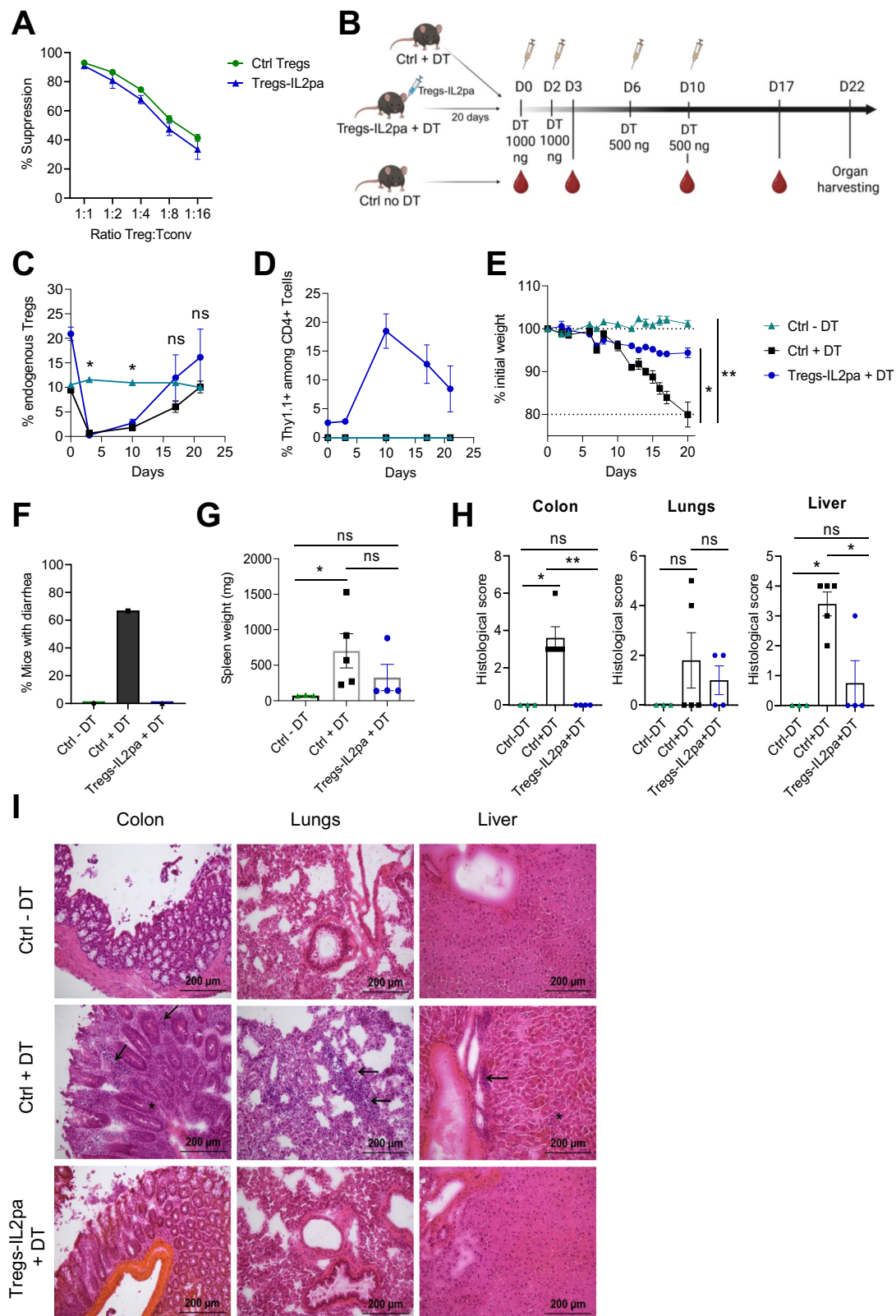
The expansion of the transferred Tregs-IL2pa was accompanied by a concomitant expansion of endogenous Tregs. This indicates that Tregs-IL2pa express more IL-2pa than they need and that this IL-2pa is then used by endogenous Tregs. As the IL-2pa has reduced biological activity, it has no significant effect on Tconv or NK cells. Over time, excess IL-2pa generates mice with an overall very large Treg compartment of even more than 50% of CD4 cells, of which about 10% were Tregs-IL2pa. This could be advantageous in situations of very strong inflammation, such as chronic GVHD, but could also be problematic in the long term. However, it is unlikely that Tregs-IL2pa expansion will show the same kinetics in humans. Firstly, as Treg proliferation requires both TCR and IL-2 stimulation, this should only occur when Tregs see their antigen, likely in lymph nodes. Thus, to proliferate, a

Tregs-IL2pa specific for a tissue-specific antigen has to enter the tissue-draining lymph node, which would occur at a lower frequency for Tregs circulating in a 75,000 cm³ human body than in a 30 cm³ mouse body and the time required to scan larger lymph nodes will also be longer. Secondly, like most biological processes, the cell cycle duration of T cells is slower in humans than in mice. Human T cells have a cell cycle duration of about 24 to 28 h, whereas mouse T cells have a cell cycle duration of about 8 to 12 h³⁸. Third, the level and kinetics of Treg expansion could be tuned by the number of Treg-IL-2pa injected and by using weaker promoters to drive IL-2pa expression. Taken together, the expansion levels of Tregs-IL2pa observed over months in mice could translate into similar expansion levels over years in humans. It should also be emphasized that the use of CAR-Tregs-IL2pa or allogeneic Tregs-IL2pa would not lead to long-term stimulation and expansion. We believe that the level of expansion observed in our experimental context will likely be much reduced in real-world applications, as this will depend heavily on the specific context of use. For example, the expansion of CAR-Tregs-IL2pa will be influenced by the frequency and intensity of CAR-mediated stimulation, while the expansion of allogeneic cells should be limited by their ablation due to the allogeneic response. Therefore, the persistence of Tregs-IL2pa will be a critical biological parameter to monitor in first-in-man clinical trials.

It is important to note that a high number or proportion of Tregs is not associated with a strong immunosuppression. We have previously generated mice that produce IL-2 continuously after the administration of an IL-2-producing AAV. After months of exposure to IL-2, this resulted in mice with more than 40% of Tregs. We showed that these mice were healthy, could mount an immune response against vaccination and infection, and did not have an increased incidence of chemically-induced tumors³⁹.

In any case, the incorporation a kill switch for conditional cell killing should allow full control of an unwanted Treg expansion level. Among the currently used kill-switches, membrane molecules with no biological activity such as tEGFR, RQR8, or CD20, for which there exist clinically used depleting monoclonal antibodies^{27–29}, are classically used in human. These molecules are also convenient to track the injected cells in patients. In this work, we used the Thy1.1 as a surrogate suicide gene and showed that Tregs-IL2pa could be efficiently ablated, even when they already represented a very large population. Moreover, the depletion appeared complete as we did not detect the reappearance of Tregs-IL2pa over months of follow-up. Altogether, the improved survival of Tregs-IL2pa and their recruitment of endogenous Tregs should translate into a need for less cells to be administered, solving the production issue.

Tregs-IL2pa maintained a stable and activated phenotype over time. Even after very long follow up, we never detected any loss of



Foxp3 nor of other Treg markers. Actually, the Tregs-IL2pa phenotype remained that of activated Tregs, with high expression of activation markers such as CD25, CTLA4, and GITR. In line with this phenotype, Tregs-IL2pa had a complete TSDR demethylation pattern, which was also the case for expanded endogenous Tregs. Moreover, Tregs-IL2pa could efficiently control the extreme inflammatory environment of the Treg depletion-induced multiorgan autoimmunity, underscoring the

stability of the Treg phenotype of Tregs-IL2pa. Therefore, IL-2pa-sufficient Tregs (now referred to as is.Tregs) address not only the production and survival of the Treg cell product, but also the stability of the Treg phenotype.

is.Tregs have a polyclonal and diverse TCR repertoire. This diversity is supported by the control of the broad autoimmunity induced by Treg depletion, which underscores that the is.Treg TCR

Fig. 4 | Murine IL-2pa-self-sufficient Tregs are suppressive in vitro and in vivo.

A In vitro suppression assay. The percentage of suppression represents Tconv inhibition of proliferation by Tregs. Transduced Tregs were sorted three days post-transduction for the experiment ($n = 2$ per group). **B** Schematic design of the autoimmunity induction experiment in twelve- to twenty-week-old male B6 Foxp3^{DTR} Thy1.2 mice expressing the diphtheria toxin receptor (DTR) in endogenous Tregs. Negative control mice did not receive Tregs and were not treated with diphtheria toxin (DT) ($n = 4$), positive control mice did not receive Tregs and were treated with DT ($n = 6$), Tregs-IL2pa mice received a 9×10^5 injection of Tregs-IL2pa and were treated with DT 20 days post-injection ($n = 6$). Mice were weighed at least three times per week and were bled on days 3, 10, and 17 for flow cytometry analysis. Data are pooled from two independent experiments. Schematic created in BioRender⁴⁹. **C** Follow-up of endogenous CD4 Tregs and **D** injected cells in the blood. Statistically significant differences were observed in the percentage of endogenous Tregs between DT-untreated and treated control mice on days 3 and 10 ($p = 0.0357$). **E** Mice weight follow-up during the autoimmunity experiment. Statistically significant differences were found between DT-untreated control mice and treated mice ($p = 0.0095$), as well as between DT-treated control mice and DT-treated mice receiving Tregs-IL2pa ($p = 0.0260$). **F** Percentage of mice with diarrhea

and **G** spleen weights at the end of the autoimmunity induction experiment on day 22. Spleen weights were significantly higher in DT-treated control mice compared to DT-untreated mice ($p = 0.0357$). **H** Histological score corresponding to the sum of grades assigned for lymphocyte infiltration in each organ. Statistically significant differences were observed in the colon between DT-treated control mice and untreated mice ($p = 0.0179$) and between DT-treated control mice and mice receiving Tregs-IL2pa ($p = 0.0079$). In the liver, a statistically significant difference was observed between DT-treated control mice and untreated mice ($p = 0.0357$), as well as between DT-treated mice and mice that received Tregs-IL2pa ($p = 0.0397$). **I** Representative images of hematoxylin and eosin-stained sections of the colon, lungs, and liver at 200 \times magnification. One slide per group and per organ was analyzed, with $n = 3$ in the Ctrl without DT group, $n = 5$ in the Ctrl with DT group, and $n = 4$ in the Tregs-IL2pa with DT group. In the colon, the arrows indicate inflammatory cell infiltration, and the star indicates crypt regeneration. In the lungs, the arrows indicate interstitial lymphocytic infiltrate. In the liver, the arrow indicates lymphocytic infiltrate in a portal tract and the star indicates intrasinusoidal lymphocytic infiltrate. Data are expressed as mean \pm SEM in the panels (**A**, **C**, **D**, **E**, **G**, **H**) and compared using a two-tailed Mann-Whitney test in the panels (**C**, **E**, **G**) and (**H**) ($^*p < 0.05$; $^{**}p < 0.01$; $^{***}p < 0.001$, $^{****}p < 0.0001$).

repertoire allows for controlling autoreactive effector T cells with multiple specificities. This polyclonal and diverse TCR repertoire is important for situations in which is.Tregs could be used as polyclonal cell populations, like for the treatment of GVHD, and less important when using Tregs that will be further engineered with targeting moieties such as CARs or TCRs.

Human is.Tregs had properties very similar to those of murine ones, although their behaviour could only be tested in the artificial setting of xenogeneic immunodeficient mice. Human is.Tregs had a much-improved survival in a setting that is almost completely devoid of endogenous IL-2 and despite the fact that their antigenic stimulation is suboptimal in the context of xenogeneic MHC molecules. Nevertheless, their functional efficacy could be demonstrated both in vitro and in the classical model of xenogeneic GVHD.

In summary, our work demonstrated the dramatically improved properties of is.Tregs that circumvent the 3 main limitations of Treg cell therapies, i.e. manufacturing, stability, and durability.

Methods

Plasmids and lentiviral vector production

Second-generation lentiviruses were utilized to generate human Tregs-IL2. The human Treg-IL2 transfer plasmids were designed and ordered from VectorBuilder's website. These transfer plasmids contained the selected partial agonist form of IL-2 linked to the enhanced green fluorescent protein (EGFP) reporter through a self-cleaving 2A peptide. Both transgenes were under the control of the human elongation factor 1 α (EF1 α) promoter. The control plasmid vector, derived from the HIV-1 self-inactivating (SIN) vector backbone pRRL-SIN18-cPPT-hPGK-EGFP-WPRE, was kindly provided by L. Naldini (Torino, Italy). The hPGK promoter was removed and replaced by ligation at the Cla-I/Bam-HI sites by the 1376 bp insert from the pEF-BOS plasmid that corresponds to the EF1 α promoter⁴⁰. The packaging construct pCMV9 (gift from D. Trono, University of Geneva, Geneva, Switzerland) and the pHCMV-VSV-G plasmid (pVSVG), encoding the vesicular stomatitis virus envelope G protein (VSV-G)⁴¹, were used to produce the recombinant vectors.

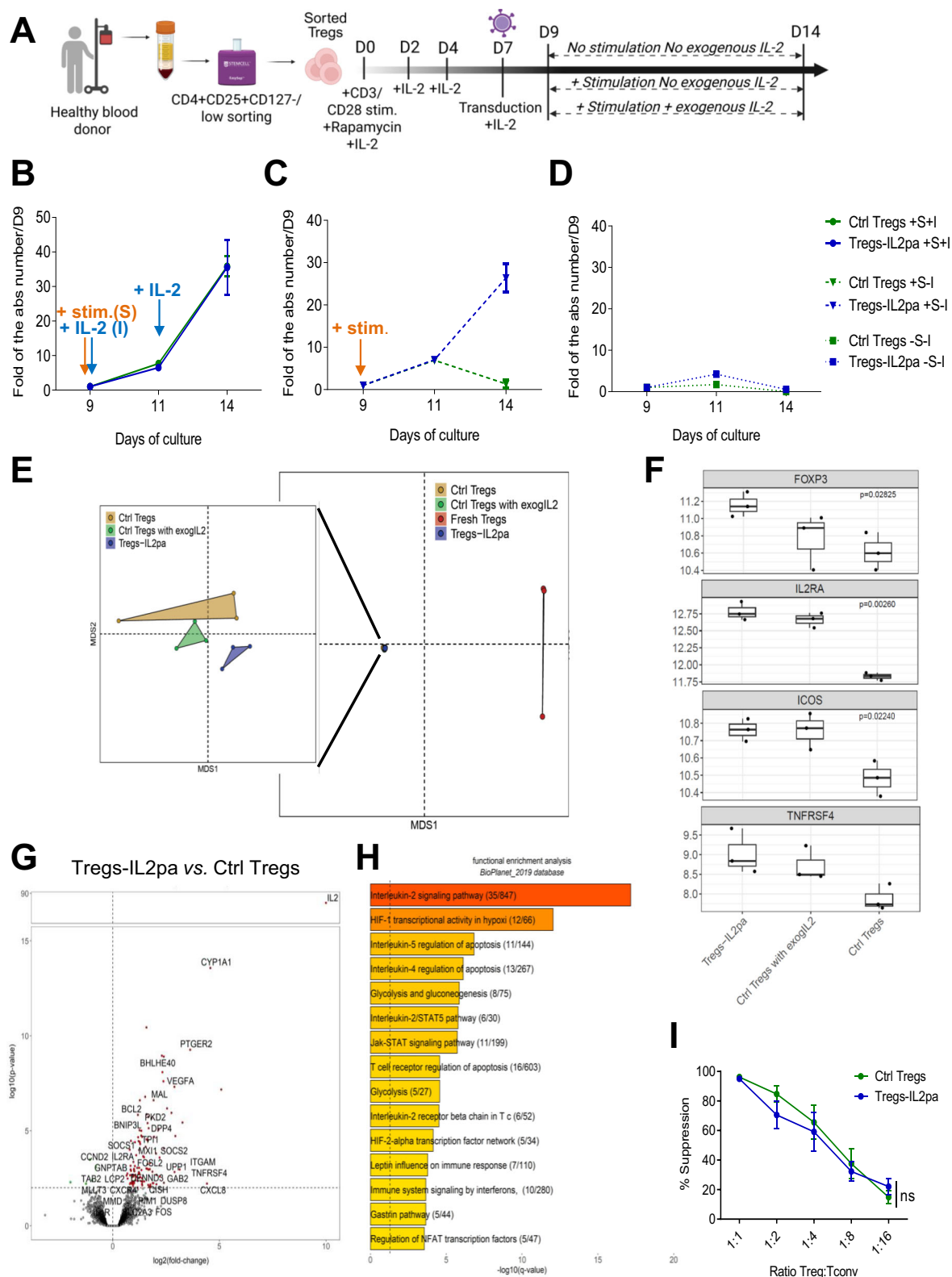
Lentiviral particles pseudotyped with the VSV-G envelope were produced by transient transfection of 293 T cells from the American Type Culture Collection (ATCC) (#CRL-11268). Cells were seeded one day before transfection at 15×10^6 cells per flask (175 cm²) in 25 mL of Dulbecco's Modified Eagle's Medium (DMEM) supplemented with high glucose (4500 mg/L), 10% heat-inactivated fetal bovine serum (FBS) (Sigma), 0.29 mg/mL L-glutamine (Glu), 100 U/mL penicillin (P), and 100 μ g/mL streptomycin (PS) (Sigma), referred to as

complete DMEM. The cells were then incubated at 37 °C in a humidified 5% CO₂ atmosphere. Transfection was performed with polyethylenimine (PEI) (PEI MAX MW 40,000, Polysciences, #49553-93-7) by first preparing two solutions: the deoxyribonucleic acid (DNA) mixture containing 29.0 μ g of transfer plasmid, 23.3 μ g of pCMV9, and 4.5 μ g of pVSVG in 2.5 mL of DMEM PSGlu (without FBS) per flask, and the PEI mixture containing 170.4 μ g of PEI in 2.5 mL of DMEM PSGlu per flask. After gentle homogenization, the PEI solution was added gently to the previously vortexed DNA solution, and the resulting mixture was vortexed for 20 seconds at the lowest intensity. After 30 min of incubation at room temperature, the solution with formed DNA-PEI complexes was gently added to the cells, 5 mL per 175 cm² flask. Transfected cells were incubated at 37 °C overnight. After 16 h, the medium was replaced with 17 mL/flask of DMEM PSGlu supplemented with 10 mM sodium pyruvate (Gibco), 10 mM sodium butyrate (Sigma Aldrich), and 0.1 mM non-essential amino acids (Gibco). After 24 h, the medium was collected and filtered with a 0.45 μ m stericup (Merck, #SCHVU01RE). Lentiviral vectors were then concentrated in a sterilized centricon 70 (Merck, #UFC710008) by centrifugation at 3300 g at 4 °C for at least 15 min until the medium left does not exceed the columns. The concentrated lentiviral vectors were collected, and the columns were washed by the addition of 1x Dulbecco's Phosphate Buffered Saline (PBS) (Sigma) and centrifugation at 800 g for 5 min at 4 °C. Lentiviral concentrates were then diluted in PBS and ultracentrifuged at 20,000 g for 90 min at 4 °C (Beckman Coulter, OptimaXE-90, rotor SW 32 Ti). After removal of the supernatant, pellets were rehydrated in PBS for 1 h at 4 °C, aliquoted, and stored at -80 °C.

Plasmids and gammaretroviral vector production

Murine stem cell viruses (MSCV) were utilized to generate mouse Tregs-IL2. All transfer plasmids were custom-designed and ordered from VectorBuilder's website. These plasmids contained either the human wild-type IL-2 (wtIL-2) or the partial-agonist version of IL-2 (IL-2pa), both optimized in their codon sequence for *Mus musculus* using the GeneArt tool from ThermoFisher. The IL-2 sequences were linked to the murine Thy1.2 (or CD90.2) reporter through a self-cleaving 2A peptide, and both transgenes were under the control of the MSCV promoter.

MSCV retroviruses were produced following a published method with some modifications^{42,43}. Briefly, the Platinum-E (Plat-E) retroviral packaging cell line (Cell Biolabs, #RV-101) was cultured and transfected in complete DMEM supplemented with 10 μ g/mL blasticidin and 1 μ g/mL puromycin (ThermoFisher). Cells were seeded at 14×10^6 cells per 175 cm² flask one day before transfection.



Transfection was performed using JetPRIME solutions (Polyplus, #101000046), utilizing 10 μ g of transfer plasmid, 60 μ l of JetPRIME reagent, and 1 mL of JetPRIME buffer per 175 cm^2 flask. After 6 h, the medium was replaced with 20 mL of fresh complete medium. Viruses were collected 48 h post-transfection, filtered using a 0.45 μ m filter, and concentrated 40 times using an Amicon Ultra 100 kD centrifugal filter (Merck, # UFC910024). The concentrated viruses were then aliquoted and stored at -80°C .

Isolation, culture, and transduction of human Tregs

Leukapheresis samples were collected from healthy blood donors at Saint Antoine and Saint Louis hospitals (Etablissement Français du Sang, Paris, France). Peripheral blood mononuclear cells (PBMCs) were separated using a Ficoll-Hypaque gradient (density 1.077 g/mL, Sigma), and $\text{CD4}^+\text{CD25}^+\text{CD127}^{\text{low}}$ Tregs were isolated from PBMCs using magnetic-activated cell sorting (EasySep kit, STEMCELL Technologies, #18063). Purified Tregs were cultured in ImmunoCult medium

Fig. 5 | In vitro characterization of human Tregs-IL2pa. **A** Schematic design of the in vitro survival assay. Schematic created in BioRender⁴⁹. Sorted Tregs were cultured and transduced on day 7 with lentiviruses to generate Ctrl Tregs (production of GFP alone) and Tregs-IL2pa (production of the IL-2 partial agonist and GFP). On day 9, unsorted transduced cells (approximately 35% of transduced cells for both vectors), were cultured in fresh medium under three different conditions: **B** with a CD3/CD28 restimulation on day 9 and addition of exogenous IL-2 on days 9 and 11, **C** with a restimulation and without the addition of IL-2, and **D** without restimulation and without the addition of exogenous IL-2. Data were obtained from two different experiments ($n = 2$ per group). **E** Multidimensional scaling (MDS) representation illustrating the similarities and differences in gene expression profiles between fresh and cultured Tregs from three different blood donors. The proximity of the dots reflects the degree of similarity in their transcriptomic profiles. Convex hulls delineate each condition. Tregs were obtained from three different donors ($n = 3$). **F** Boxplot showing the gene expression levels of some Treg activation and functional markers ($n = 3$). **G** Volcano plot illustrating differential

gene expression between transduced sorted Ctrl Tregs and Tregs-IL2pa. Genes upregulated in Ctrl Tregs are shown in green, while those upregulated in Tregs-IL2pa are shown in red. **H** Bar plot illustrating the results of functional enrichment analysis. Each horizontal bar represents a biological pathway from the BioPlanet database, with the length proportional to its statistical significance, indicated by the $-\log_{10}$ of the p-value. **I** In vitro suppression assay. Data were extracted from two separate experiments ($n = 6$ per group). Data are presented as mean \pm SEM in panels (**B–D**), and (**I**), with comparisons performed using a two-tailed unpaired t-test in panel (**F**) and a two-tailed Mann–Whitney test in panel (**I**) ($*p < 0.05$; $**p < 0.01$; $***p < 0.001$, $****p < 0.0001$). The boxplots in panel (**F**) show the median (Q2) as the central line, the first and third quartiles (Q1 and Q3) as the bounds of the box, and whiskers extending to 1.5 times the interquartile range; points beyond are outliers. For panel (**G**), differential expression analysis was performed using DESeq2 with two-sided tests and unadjusted p-values. For panel (**H**), statistical analysis was performed using a two-sided Fisher's exact test, and p-values were adjusted for multiple comparisons.

(STEMCELL Technologies, #10981) supplemented with 1% Penicillin–Streptomycin–L–Glutamine (Sigma), 300 International Units (IU)/mL of IL-2 from ILTOO Pharma (ILT-101), 100 nM of rapamycin (LCIabs), and 25 μ L/mL of Immunocult anti-CD3/anti-CD28 T cell activator (STEMCELL Technologies, #10971). Fresh medium was added every two to three days to maintain a concentration of $2\text{--}2.5 \times 10^5$ cells/mL supplemented with 300 U/mL of IL-2 in the total volume.

Tregs were transduced on day 7 or 9 at a multiplicity of infection (MOI) of 1 with 8 μ g/mL of protamine sulfate (Wockhardt). Cells were spinoculated for 30 min at 1000 g at 32 °C. Transduction efficiency was determined two days post-transduction and monitored at different time points by flow cytometry.

Isolation, culture, and transduction of mouse Tregs

Mouse Tregs were obtained from B6 Foxp3^{EGFP} Thy1.1 mice sourced from spleens and lymph nodes (brachial, cervical, axillary, and inguinal). The organs were dissociated using the Gentle MACS system (Miltenyi) and enriched in CD4 cells using a CD4 enrichment kit (STEMCELL Technologies, #19852 A). CD4⁺Foxp3-GFP⁺ cells were subsequently sorted by fluorescence-activated cell sorting (FACS) using the FACS Aria II system (BD Biosciences). Mouse Tregs were cultured according to a published protocol⁴³, with some modifications. Cells were stimulated with anti-CD3/CD28 Dynabeads (ThermoFisher, #11453D) at a 1:2 Tregs to beads ratio and maintained at a concentration of 1.5×10^5 cells/mL. Transductions were performed on day 5 at a MOI of 0.05 with 8 μ g/mL of protamine sulfate, with a 30-minute spinoculation at 1000 g at 32 °C. On day 7, transduction efficacy was assessed, and beads were removed in preparation for either cell injection or further in vitro experiments.

Antibodies and flow cytometry analysis

Antibodies used for human and murine cell stainings are listed in Supplemental Table 1. Human Foxp3 stainings were performed using the PERFIX-NC kit (Beckman Coulter, #B31167) and the staining buffers for Foxp3/transcription factor (ThermoFisher, #00-5523-00) for mouse Tregs following the manufacturer's instructions. Intracellular phosphorylated STAT-5 staining was performed using the PERFIX-Expose kit (Beckman Coulter, #B26976) according to the manufacturer's instructions. Flow cytometry analyses were conducted on a Cytotex LX instrument (Beckman Coulter), and data were analyzed using FlowJo 10.6.1 software (BD Biosciences).

Suppression assays

In human Treg-based assays, GFP⁺ transduced cells were sorted three days post-transduction and co-cultured with autologous Tconv. CD4⁺CD25⁺ Tconv cells were obtained following the manufacturer's instructions for optional CD4⁺CD25⁺ sorting using the CD4⁺CD25⁺CD127

kit (STEMCELL Technologies, #18063). Tconv cells were frozen on the day of Treg sorting and thawed for suppressive assays. Prior to co-culture, Tconv cells were stained with CellTrace Violet (ThermoFisher, #34557) following the manufacturer's instructions and seeded at 5×10^4 cells/well with 1 μ L of ImmunoCult Human CD3/CD28 T Cell Activator (STEMCELL Technologies, #10971). Sorted Tregs were mixed with Tconv at ratios of 1/1, 1/2, 1/4, 1/8, and 1/16 Tregs/Tconv. Tconv proliferation, illustrated by CellTrace Violet profiles, was assessed after 4 days by flow cytometry.

In murine Treg-based assays, transduced Thy1.2⁺ cells were sorted three days post-transduction. Fresh CD4⁺CD25⁺ Tconv cells were isolated from splenocytes of B6 Foxp3^{EGFP} Thy1.1 mice and sorted by FACS as CD4⁺Foxp3GFP⁺ cells. Tconv cells were also stained with CellTrace Violet for proliferation monitoring and seeded at 5×10^4 cells/well with anti-CD3/CD28 Dynabeads (1 bead:1 Tconv). Transduced-sorted Tregs were co-cultured at ratios of 1/1, 1/2, 1/4, 1/8, and 1/16 Tregs/Tconv, and cells were analyzed 4 days later.

In vitro survival assay with human Tregs

Two days post-transduction, non-sorted transduced cells were resuspended in fresh medium and cultured under three different conditions, with 1×10^5 cells per condition, for five days. The first culture group was not restimulated and did not receive exogenous IL-2. The second group received 25 μ L/mL of Immunocult anti-CD3/anti-CD28 T cell activator (STEMCELL Technologies, #10971) but not exogenous IL-2. The third group was restimulated and received 300 IU/mL of IL-2. Cells were counted every two days and supplemented with fresh medium to maintain a concentration of $2\text{--}2.5 \times 10^5$ cells/mL, with IL-2 added every two days to the corresponding condition.

Mice

Male and female mice aged six to twenty weeks were used in the experiments. All were bred in-house at the New Common Animal Facility at Pitié Salpêtrière Hospital, with the conventionally controlled status, except for the B6.Cg-Rag2^{tm1.1Cgn}/J (RAG) mice, which were bred at the UMS28 Animal Facility at Charles Foix Hospital, with the Specific Opportunist Pathogen Free (SOPF) status. Mice used for the experiments were transferred to the UMS28 experimental animal facility, with a conventionally controlled status, at Pitié Salpêtrière Hospital. B6.129(Cg)-Foxp3^{tm3(Hbegf/GFP)Ayr}/J, referred to as B6 Thy1.2 were used as recipient mice for mouse Tregs (Jackson Laboratory, #016958). These mice have endogenous Foxp3-GFP Tregs that also express the Diphtheria Toxin Receptor (DTR) and the congenic marker Thy1.2. B6 Foxp3^{EGFP} Thy1.1, referred to as B6 Thy1.1, were used as donor mice for Treg and Tconv isolation. These mice were generated by crossing B6.Cg-Foxp3^{tm1Kuch}/J (#035864), referred as B6 Foxp3-GFP and B6.PL-Thy1^a/CyJ (#000406), both obtained from Jackson Laboratory. Murine Tregs were also injected in six to seven-

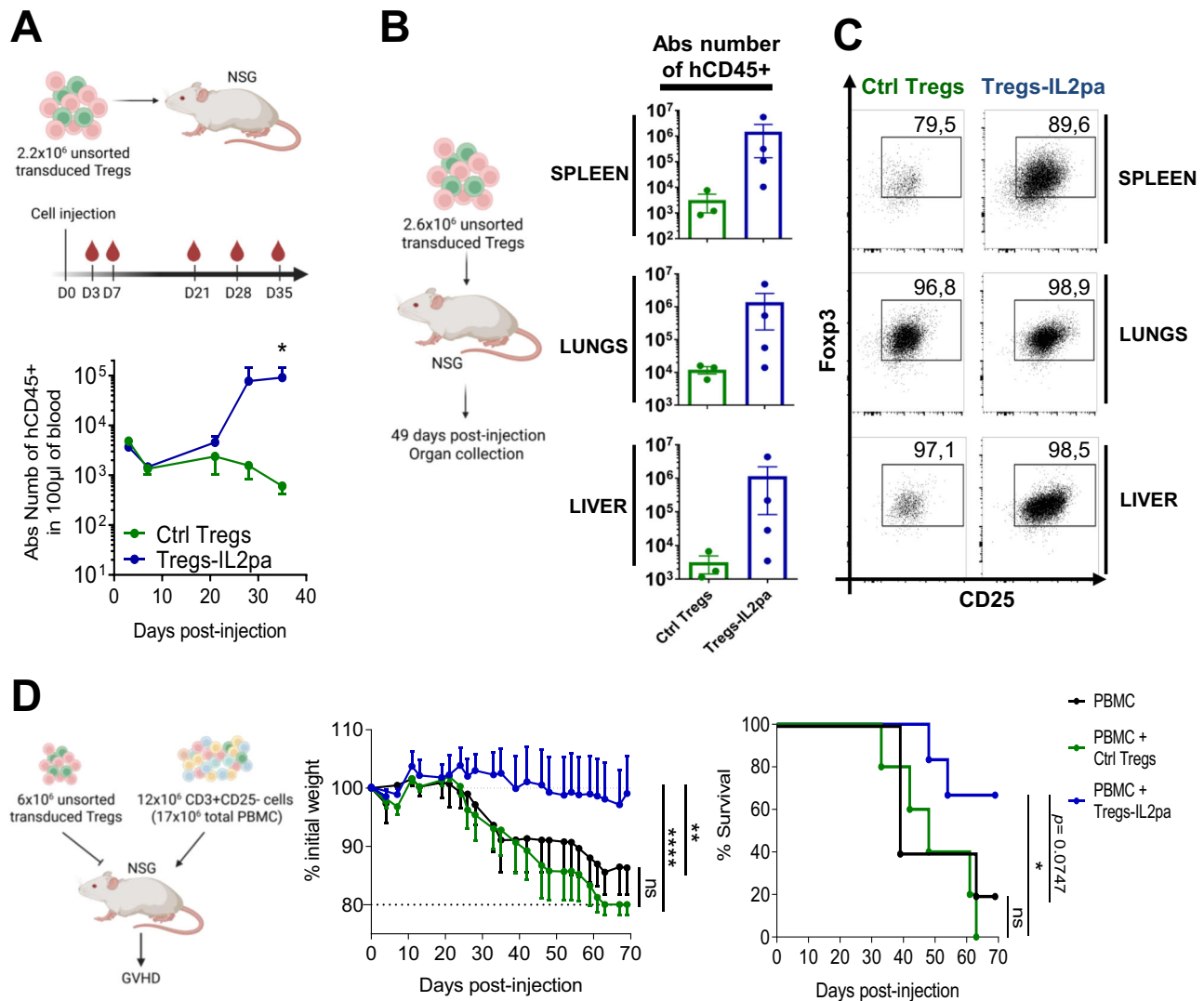


Fig. 6 | Human Tregs-IL2pa have long-term survival and exert robust suppressive activity in immunodeficient recipient mice. A Dynamics of the absolute number of injected human CD45⁺ cells in 100 µL of blood. Six- to twenty-week-old male and female NSG mice received 2.2×10^6 unsorted, transduced control Tregs (Ctrl Tregs, $n = 3$) or Tregs-IL2pa ($n = 6$) with 9% transduced cells in both groups. Cell survival was evaluated in blood samples. On day 35, the number of injected cells in the blood was significantly higher in mice that received Tregs-IL2pa compared to those receiving Ctrl Tregs ($p = 0.0238$). Schematic created in BioRender⁴⁹. **B** Absolute numbers of injected human CD45⁺ cells in NSG spleen, lungs, and liver. Mice received 2.6×10^6 unsorted transduced Ctrl Tregs ($n = 3$) or Tregs-IL2pa ($n = 4$) with 5% transduced cells in both groups. Cell survival was assessed 49 days post-injection in the organs. Schematic created in BioRender⁴⁹. **C** Representative dot plots showing the expression of CD25 and FcγR3 in injected cells. **D** Suppression of cell-mediated xenogeneic graft-versus-host disease (xeno-GVHD). Eight- to twenty-

week-old male and female NSG mice received either 12×10^6 CD3⁺CD25⁻ cells alone (PBMC, $n = 5$) or combined with 6×10^6 unsorted autologous transduced Ctrl Tregs ($n = 5$) or Tregs-IL2pa ($n = 6$), with approximately 70% of transduced cells in each vector. Mouse weights were monitored every two days and are depicted on the left. Schematic created in BioRender⁴⁹. Statistically significant differences were observed in the weight of mice receiving Tregs-IL2pa compared to those receiving PBMC only ($p = 0.0013$) and those receiving Ctrl Tregs ($p < 0.0001$). Survival curves for xeno-GVHD are presented on the right. The survival rate was significantly higher in mice that received Tregs-IL2pa compared to those that received Ctrl Tregs ($p = 0.0428$). Data are presented as mean \pm SEM in panels (A), (B), and (D) and were analyzed using a two-tailed Mann-Whitney test for panels (A) and (B). In panel (D), a Kruskal-Wallis test was used for weight analysis, and a Gehan-Breslow-Wilcoxon test was used for survival curve comparisons. (* $p < 0.05$; ** $p < 0.01$; *** $p < 0.001$, **** $p < 0.0001$).

week-old male B6.Cg-Rag2^{tm1.1Cgn}/J, referred to as RAG mice (Jackson Laboratory, #008448). NOD.Cg-Prkdc^{scid} IL2rg^{tm1Wjl}/SzJ or NSG mice, were used as recipients for human Tregs (Jackson Laboratory, #005557). Human cells were injected into male or female NSG mice. For murine cells, when the donor mice were female, the cells were injected into female recipient mice, and vice versa. The animals were housed in ventilated racks with an automatic watering system and ad libitum access to food. Temperature and humidity conditions are controlled and monitored. The lighting cycle is 12 h per day (6 AM - 6 PM). The animals are housed with their conspecifics (maximum of 5

per cage). At the end of the experiments, mice were euthanized by cervical dislocation.

Adoptive transfer of human Tregs in NSG mice

Transduced non-sorted Tregs were injected intravenously into six to twenty-week-old male and female NSG mice at a dose of 2.2 – 2.6×10^6 cells per mouse. Cell survival was assessed in blood or in organs at the time of euthanasia, 49 days post-injection. Spleens, lungs, and livers were collected to evaluate Treg survival. Lung and liver tissues were dissociated using the corresponding dissociation kit following the

manufacturer's instructions (Miltenyi, #130-095-927 and #130-105-807).

Xenogeneic Graft-versus-Host Disease

Xenogeneic graft-versus-host disease (GVHD) was induced by intravenous injection of human CD25⁺ depleted peripheral blood mononuclear cells (PBMCs) in eight to twenty-week-old male and female NSG mice. Each mouse received 12×10^6 CD3⁺ CD25⁺ cells per mouse. CD25⁺ depleted PBMCs were obtained using the CD4⁺CD25⁺CD127⁺ sorting kit (STEMCELL Technologies, #18063) following the optional CD4⁺CD25⁺ sorting protocol without the CD4 enrichment step. Two days post-transduction, transduced non-sorted Tregs (6×10^6 per mouse) were concomitantly injected with autologous PBMCs at a final 1/2 Treg/CD3⁺CD25⁺ ratio. NSG mice developed severe xenogeneic GVHD within 4–5 weeks. Mice were monitored three times per week for weight loss and were euthanized when they lost $\geq 20\%$ of their initial body weight.

Adoptive transfer of murine Tregs: survival, dose testing, blood transfer, and depletion studies

Cultured and transduced non-sorted Tregs from B6 Thy1.1 mice were injected intravenously into B6 Thy1.2 mice at a dose of 9×10^5 cells per mouse. Some mice were euthanized 14 days post-injection to assess Treg survival in the blood, spleen, lungs, and liver. Lung and liver tissues were dissociated using the appropriate dissociation kits according to the manufacturer's instructions (Miltenyi, #130-095-927 and #130-105-807). Blood samples were collected from the remaining mice at least once every two weeks for 4 to 6 months to monitor cell expansion.

AAV vectors for AAV-IL2 injection were produced by the ViVeM Center, Inserm UMR1089, in Nantes. AAV2/8 vectors encoding human wild-type IL-2 were purchased and injected intraperitoneally in B6 Thy1.2 mice at a dose of 1×10^{11} viral genome (vg) in 100 μ L on the same day as the cell injection.

Additionally, mice that received an intravenous injection of 1×10^5 non-sorted Tregs-IL2pa were similarly followed for blood collection at least once every two weeks for up to 4 months.

Intravenous blood transfers of 250 μ L were performed from a B6 Thy1.2 mouse that had received 3×10^5 non-sorted Tregs-IL2pa 10–11 months before, to fresh unmanipulated B6 Thy1.2 mice. Cell survival was assessed every 7 to 14 days in the blood of the new recipients.

For depletion of Thy1.1 injected cells, mice received a single intraperitoneal injection of 250 μ g of depleting anti-Thy1.1 antibody (BioXCell, #BE0214) 133 days after the injection of 9×10^5 non-sorted Tregs-IL2pa. The suppression of injected cells was monitored 7 days post-treatment in the blood, and mice were followed for up to 2 months post-treatment to control for cell depletion.

For cell injections into six to seven-week-old male RAG mice, cultured and transduced non-sorted Tregs from B6 Thy1.1 mice were administered intravenously and monitored in blood samples every 7–14 days.

Autoimmunity induction model

Twelve to twenty-week-old male B6 Thy1.2 (B6.129(Cg)-Foxp3^{tm3(HbeGFP)Ayr/J}) were administered 9×10^5 Tregs-IL2pa per mouse twenty days prior to the induction of autoimmunity. Autoimmunity was induced through endogenous Treg depletion, with the mice receiving an initial intraperitoneal (IP) injection of 1000 ng diphtheria toxin (DT) (Sigma) on day 0. This was followed by a second DT IP injection of 1000 ng on day 2 and two subsequent injections of 500 ng each on days 6 and 10. The survival of injected cells and depletion of endogenous Tregs were monitored in the blood on days 0, 3, 10, and 17. As a control, one group of mice was treated with DT but did not receive a Treg injection, and another group neither received Tregs nor DT treatment. Mice were monitored three times per week for weight loss and were euthanized

when they lost $\geq 20\%$ of their initial body weight. On day 22, mice were euthanized, and the colon, liver, and lungs were collected and frozen in OCT embedding matrix (CellPath) for further histological analysis. Sections of 10 μ m were prepared and stained with hematoxylin and eosin (H&E) for lymphocyte infiltration analysis. A pathologist blindly scored the slides on a score from 0 to 2. For the colon, five parameters were considered (apoptosis of the crypts, regeneration of the crypts, loss of crypts, chorion inflammation, and mucosal ulceration), three parameters were assessed for the lungs (periluminal, interstitial alveolar, and extensive lesions), and seven parameters for the liver (portal lymphocytic infiltrate, biliary ducts, endothelitis, periportal necrosis, acidophilic bodies, confluent necrosis, and sinusoidal lymphocytosis). The sum of the scores for each organ constituted the global histological score reported for each organ.

Transcriptomic analysis from human Tregs

Human Tregs were isolated from healthy donors. Leukapheresis samples were collected at Saint Antoine and Saint Louis hospitals (Etablissement Français du Sang, Paris, France). Peripheral blood mononuclear cells (PBMCs) were separated using a Ficoll-Hypaque gradient (density 1.077 g/mL, Sigma), and CD4⁺CD127^{low}CD25⁺ Tregs were isolated from PBMCs using magnetic-activated cell sorting (EasySep kit, STEMCELL Technologies, #18063). From the freshly isolated Tregs, 1.5×10^5 cells per donor were collected and lysed for RNA extraction (Qiagen, #80004), while the remaining cells were cultured. On day 11 of culture, two days post-transduction, both transduced Ctrl Tregs and Tregs-IL2pa were cultured in fresh medium without exogenous IL-2 for a 3-day IL-2 resting period. As a control, only one well of Ctrl Tregs was replenished with IL-2. On day 14, 1.5×10^5 transduced GFP⁺ cells from each condition were sorted using FACS Aria II (BD Biosciences) and subsequently lysed for RNA extraction (Qiagen). RNA library preparation were realized following manufacturer's recommendations (NEBnext rRNA depletion #E6310 + Ultra II Directional RNA kit #E7760L from New England Biolabs). Final samples pooled library prep were sequenced on ILLUMINA novaseq 6000 with SP-200 cartridge (2x800Millions of 100 bases reads), corresponding to 2x30 million reads per sample after demultiplexing. For data analysis, reads were aligned to the GRCh38.p14 release of the human gene transcriptome using Salmon software (version 1.10⁴⁴). Multidimensional scaling (MDS) was generated based on the whole transcriptome. Differentially expressed genes were identified using DESeq2⁴⁵, based on a p-value threshold of 0.01 and a log2 fold change threshold of 1.2. Functional enrichment analysis was conducted using Enrich R⁴⁶ and the Bioplanet database⁴⁷.

Bulk TCR analysis from mouse Tregs

Four to six months after the injection of 9×10^5 Tregs-IL2pa into B6 Thy1.2 mice, the animals were euthanized to collect spleens for cell sorting. Both injected and endogenous Treg cells were sorted from Tregs-IL2pa mice, while naïve (CD4⁺Foxp3GFP⁺CD44^{CD62L}⁺) and activated memory Tregs (CD4⁺Foxp3GFP⁺CD62L^{CD44}^{high}) were sorted from unmanipulated C57BL/6 female mice using FACS Aria II (BD Biosciences). Subsequently, the cells were lysed for RNA extraction using the RNeasy RiboZero Total Isolation Kit (Invitrogen, #AM1912). TRA and TRB libraries were prepared on 100 ng of RNA with the SMARTer Mouse TCR a/b Profiling Kit v1 (Takara Bio, # 634403) and sequenced with MiSeq Reagent Kit v3 paired-end reads (2 x 300 bp) (Illumina) plus 10% PhiX at the ICM genotyping/sequencing Platform. Raw data in FASTQ format were processed for TRB sequence annotation using MiXCR software (v3.0.3), which ensures PCR and sequencing error corrections. Amino acid CDR3 sequences with a length falling out of range (mean – 8 aa < length < mean + 8 aa) were excluded. A down-sampling to 100k sequences was performed on all samples to ensure comparability between conditions. Renyi entropy was calculated using the vegan (v2.6-2) R package to assess the diversity through a

continuum of several measures defined as α parameters. Each α considers a subset of clonotypes within a specific frequency range. For instance, at $\alpha = 0$, the Renyi value is equivalent to species richness, and is thus the entropy of the total number of clonotypes within a given sample. At $\alpha = 1$, the Shannon entropy is calculated. The higher the α , the more the Renyi index is concentrated on frequent clonotypes. The higher the Renyi entropy, the more diverse is the repertoire. Clonotype count distribution represents the proportion occupied by the clonotypes belonging to defined count intervals within the overall repertoire. All plots were generated using ggplot2 (v3.3.6).

Single-cell analysis from mouse Tregs

Six months post-injection of 9×10^5 Tregs-IL2pa to B6 Thy1.2, a 32-week-old mouse was euthanized for spleen collection and injected as well as endogenous Treg cell sorting. Tregs from an unmanipulated B6 Foxp3-GFP mouse have been sorted as control. Single-cell library construction was performed using Chromium Next GEM Single Cell 5' Library & Gel Bead kit v1.1 (#PN-1000165), Chromium Next GEM Chip G Single Cell Kit (#PN-1000127), Chromium Single Cell 5' Library construction kit (16 rxns) (#PN-1000020), and Single Index kit T set A (#PN-1000213) according to the manufacturer's protocol. Briefly, single-cell suspensions from a total of 20,000 cells with barcoded gel beads and partitioning oil were loaded to Chromium Next GEM Chip G to generate single-cell gel bead-in-emulsion. Full-length cDNA along with cell barcode identifiers were PCR-amplified to generate 5' Gene Expression (GEX) libraries. Libraries were sequenced on a NovaSeq 6000 (Illumina) to achieve a minimum of 23,000 pair-end reads per cell for GEX at the ICM genotyping/sequencing Platform. Reads were aligned using Cell Ranger v6.1.1 (10xgenomics) to the GRCm38 mouse references. Single-cell RNA sequencing data have been analysed using Seurat library⁴⁸ and RStudio (version 4.3.1).

Treg Specific Demethylated Region (TSDR) DNA methylation analysis

Secondary recipient B6 Thy1.2 mice that received a blood transfer of 250 μ L from a primary recipient B6 Thy1.2 mouse injected 11 months before with 3×10^5 non-sorted Tregs-IL2pa, were used for DNA methylation analysis. The new recipient mice were euthanized one to two months post-blood transfer for spleen collection and injected as well as endogenous CD4 Treg and Tconv sorting using the FACS Aria II (BD Biosciences). Endogenous Tregs from mice that did not receive a Treg injection, were sorted and used as controls. A total of 5×10^5 cells were sorted for endogenous cells and at least 2×10^4 injected cells. Genomic DNA extraction and bisulfite conversion were performed using EZ DNA Methylation-Direct Kit (Zymo, #D5020). Converted genomic DNA were submitted to the Hartwell Center at SJCRH for library construction and sequencing on the Illumina NovaSeq platform with 150 bp paired-end and target reads of 500 million per sample. WGBS reads were trimmed by 10 bp on 5' and 3' ends as well as all Illumina adapter sequences. Trimmed reads were aligned to the mm10 genome using the BSMAP v. 2.90 software. Methylation levels were called by methratio.py script of BSMAP. The analysis covered 14 CpGs of the Intron 1 of Foxp3 spanning from ChX: 7583799 to 7584280.

Statistical analysis

Graphing and statistical analyses were performed using GraphPad Prism 8.4.2 software (GraphPad Software). Statistical analyses were performed using the unpaired two-tailed Mann-Whitney test, unpaired t-test, Kruskal-Wallis test, or Gehan-Breslow-Wilcoxon test. The specific test used is indicated in each figure legend. Data were expressed as mean \pm SEM. Statistical significance was taken at the 5% level ($p < 0.05$), and the degree of significance was indicated as follows: * $p < 0.05$; ** $p < 0.01$; *** $p < 0.001$, **** $p < 0.0001$. Only significant

differences are shown unless non-significant differences (denoted as "ns") are specifically indicated.

Ethical approvals

Human leukapheresis products were obtained from the Etablissement Français du Sang (EFS) under the agreement n°21/EFS/024 established between EFS and our institution. Written informed consent was obtained from all healthy volunteers by EFS in accordance with ethical guidelines. The animal procedures were approved by the "Comité d'éthique en expérimentation animale Charles Darwin" registered at the "Comité National de Réflexion Ethique sur l'Expérimentation animale", CEEAACD 005, under the project agreement n°29481.

Reporting summary

Further information on research design is available in the Nature Portfolio Reporting Summary linked to this article.

Data availability

All data are included in the Supplementary Information or available from the authors, as are unique reagents used in this Article. The raw numbers for charts and graphs are available in the Source Data file whenever possible. The raw sequencing data generated in this study have been deposited in the SRA database under the accession codes: [PRJNA1248774](https://doi.org/10.1038/s41467-025-60082-z) for the human transcriptomic data and [PRJNA1250406](https://doi.org/10.1038/s41467-025-60082-z) for the murine single-cell transcriptomic data. The processed TCR sequencing data have been deposited in Zenodo database under accession code <https://doi.org/10.5281/zenodo.15183541>. Source data are provided with this paper.

References

1. Sakaguchi, S., Sakaguchi, N., Asano, M., Itoh, M. & Toda, M. Immunologic self-tolerance maintained by activated T cells expressing IL-2 receptor α -chains (CD25). Breakdown of a single mechanism of self-tolerance causes various autoimmune diseases. *J. Immunol.* **155**, 1151–1164 (1995).
2. Koreth, J. et al. Interleukin-2 and Regulatory T Cells in Graft-versus-Host Disease. *N. Engl. J. Med.* **365**, 2055–2066 (2011).
3. Raeber, M. E., Sahin, D., Karakus, U. & Boyman, O. A systematic review of interleukin-2-based immunotherapies in clinical trials for cancer and autoimmune diseases. *eBioMedicine* **90**, <https://doi.org/10.1016/j.ebiom.2023.104539> (2023).
4. Saadoun, D. et al. Regulatory T-Cell Responses to Low-Dose Interleukin-2 in HCV-Induced Vasculitis. *N. Engl. J. Med.* **365**, 2067–2077 (2011).
5. Ferreira, L. M. R., Muller, Y. D., Bluestone, J. A. & Tang, Q. Next-generation regulatory T cell therapy. *Nat. Rev. Drug Discov.* **18**, 749–769 (2019).
6. Bluestone, J. A., McKenzie, B. S., Beilke, J. & Ramsdell, F. Opportunities for Treg cell therapy for the treatment of human disease. *Front. Immunol.* **14**, 1166135 (2023).
7. Bender, C. et al. A phase 2 randomized trial with autologous polyclonal expanded regulatory T cells in children with new-onset type 1 diabetes. *Sci. Transl. Med.* **16**, eadn2404 (2024).
8. Marek-Trzonkowska, N. et al. Therapy of type 1 diabetes with CD4+CD25highCD127-regulatory T cells prolongs survival of pancreatic islets — Results of one year follow-up. *Clin. Immunol.* **153**, 23–30 (2014).
9. Trzonkowski, P. et al. First-in-man clinical results of the treatment of patients with graft versus host disease with human ex vivo expanded CD4+CD25+CD127- T regulatory cells. *Clin. Immunol.* **133**, 22–26 (2009).
10. Bluestone, J. A. et al. Type 1 diabetes immunotherapy using polyclonal regulatory T cells. *Sci. Transl. Med.* **7**, 315ra189 (2015).

11. Tang, Q. et al. Central role of defective interleukin-2 production in the triggering of islet autoimmune destruction. *Immunity* **28**, 687–697 (2008).
12. Long, S. A. et al. Defects in IL-2R signaling contribute to diminished maintenance of FOXP3 expression in CD4⁺CD25⁺ regulatory T-Cells of Type 1 diabetic subjects. *Diabetes* **59**, 407–415 (2009).
13. Pérol, L. et al. Loss of immune tolerance to IL-2 in type 1 diabetes. *Nat. Commun.* **7**, 13027 (2016).
14. Barron, L. et al. Cutting Edge: Mechanisms of IL-2-Dependent Maintenance of Functional Regulatory T Cells. *J. Immunol.* **185**, 6426–6430 (2010).
15. Setoguchi, R., Hori, S., Takahashi, T. & Sakaguchi, S. Homeostatic maintenance of natural Foxp3⁺ CD25⁺ CD4⁺ regulatory T cells by interleukin (IL)-2 and induction of autoimmune disease by IL-2 neutralization. *J. Exp. Med.* **201**, 723–735 (2005).
16. Baron, K. J. & Turnquist, H. R. Clinical Manufacturing of Regulatory T Cell Products For Adoptive Cell Therapy and Strategies to Improve Therapeutic Efficacy. *Organogenesis* **19**, 2164159 (2023).
17. MacDonald, K. N., Piret, J. M. & Levings, M. K. Methods to manufacture regulatory T cells for cell therapy. *Clin. Exp. Immunol.* **197**, 52–63 (2019).
18. Raffin, C., Vo, L. T. & Bluestone, J. A. Treg cell-based therapies: challenges and perspectives. *Nat. Rev. Immunol.* **20**, 158–172 (2020).
19. Fontenot, J. D., Gavin, M. A. & Rudensky, A. Y. Foxp3 programs the development and function of CD4⁺CD25⁺ regulatory T cells. *Nat. Immunol.* **4**, 330–336 (2003).
20. Hori, S., Nomura, T. & Sakaguchi, S. Control of Regulatory T Cell Development by the Transcription Factor Foxp3. *Science* **299**, 1057–1061 (2003).
21. Wu, Y. et al. FOXP3 Controls Regulatory T Cell Function through Cooperation with NFAT. *Cell* **126**, 375–387 (2006).
22. Bovenschen, H. J. et al. Foxp3⁺ Regulatory T Cells of Psoriasis Patients Easily Differentiate into IL-17A-Producing Cells and Are Found in Lesional Skin. *J. Invest. Dermatol.* **131**, 1853–1860 (2011).
23. Hovhannisyan, Z., Treatman, J., Littman, D. R. & Mayer, L. Characterization of interleukin-17-producing regulatory T cells in inflamed intestinal mucosa from patients with inflammatory bowel diseases. *Gastroenterology* **140**, 957–965 (2011).
24. Ueno, A. et al. Increased prevalence of circulating novel IL-17 secreting Foxp3 expressing CD4⁺ T cells and defective suppressive function of circulating Foxp3⁺ regulatory cells support plasticity between Th17 and regulatory T cells in inflammatory bowel disease patients. *Inflamm. Bowel Dis.* **19**, 2522–2534 (2013).
25. Zhou, X. et al. Instability of the transcription factor Foxp3 leads to the generation of pathogenic memory T cells in vivo. *Nat. Immunol.* **10**, 1000–1007 (2009).
26. Amouyal, C. et al. Pregnant type 1 diabetes women with rises in C-peptide display higher levels of regulatory T cells: A pilot study. *Diabetes Metab.* **47**, 101188 (2021).
27. Introna, M. et al. Genetic Modification of Human T Cells with CD20: A Strategy to Purify and Lyse Transduced Cells with Anti-CD20 Antibodies. *Hum. Gene Ther.* **11**, 611–620 (2000).
28. Kao, R. L. et al. A Cetuximab-Mediated Suicide System in Chimeric Antigen Receptor-Modified Hematopoietic Stem Cells for Cancer Therapy. *Hum. Gene Ther.* **30**, 413–428 (2019).
29. Philip, B. et al. A highly compact epitope-based marker/suicide gene for easier and safer T-cell therapy. *Blood* **124**, 1277–1287 (2014).
30. Singh, K., Hjort, M., Thorvaldson, L. & Sandler, S. Concomitant analysis of Helios and Neuropilin-1 as a marker to detect thymic derived regulatory T cells in naïve mice. *Sci. Rep.* **5**, 7767 (2015).
31. Li, D.-Y. & Xiong, X.-Z. ICOS⁺ Tregs: a functional subset of tregs in immune diseases. *Front. Immunol.* **11**, <https://doi.org/10.3389/fimmu.2020.02104> (2020).
32. Golovina, T. N. et al. CD28 Costimulation is Essential for Human T Regulatory Expansion and Function. *J. Immunol. Baltim. Md 1950* **181**, 2855–2868 (2008).
33. Levine, A. G., Arvey, A., Jin, W. & Rudensky, A. Y. Continuous requirement for the TCR in regulatory T cell function. *Nat. Immunol.* **15**, 1070–1078 (2014).
34. Vahl, J. C. et al. Continuous T Cell Receptor Signals Maintain a Functional Regulatory T Cell Pool. *Immunity* **41**, 722–736 (2014).
35. Fisson, S. et al. Continuous Activation of Autoreactive CD4⁺ CD25⁺ Regulatory T Cells in the Steady State. *J. Exp. Med.* **198**, 737–746 (2003).
36. Kim, J. M., Rasmussen, J. P. & Rudensky, A. Y. Regulatory T cells prevent catastrophic autoimmunity throughout the lifespan of mice. *Nat. Immunol.* **8**, 191–197 (2007).
37. Ho, P. et al. Harnessing regulatory T cells to establish immune tolerance. *Sci. Transl. Med.* **16**, eadm8859 (2024).
38. Baron, C. & Pénit, C. Study of the thymocyte cell cycle by bivariate analysis of incorporated bromodeoxyuridine and DNA content. *Eur. J. Immunol.* **20**, 1231–1236 (1990).
39. Churlaud, G. et al. Sustained stimulation and expansion of Tregs by IL2 control autoimmunity without impairing immune responses to infection, vaccination and cancer. *Clin. Immunol.* **151**, 114–126 (2014).
40. Dupuy, F. P. et al. Lentiviral transduction of human hematopoietic cells by HIV-1- and SIV-based vectors containing a bicistronic cassette driven by various internal promoters. *J. Gene Med.* **7**, 1158–1171 (2005).
41. Yee, J. K., Friedmann, T. & Burns, J. C. Generation of high-titer pseudotyped retroviral vectors with very broad host range. *Methods Cell Biol.* **43**, 99–112 (1994).
42. Hammill, J. A., Afsahi, A., Bramson, J. L. & Helsen, C. W. Viral Engineering of Chimeric Antigen Receptor Expression on Murine and Human T Lymphocytes. *Methods Mol. Biol. Clifton NJ* **1458**, 137–157 (2016).
43. Wu, D. et al. A method for expansion and retroviral transduction of mouse regulatory T cells. *J. Immunol. Methods* **488**, 112931 (2021).
44. Patro, R., Duggal, G., Love, M. I., Irizarry, R. A. & Kingsford, C. Salmon provides fast and bias-aware quantification of transcript expression. *Nat. Methods* **14**, 417–419 (2017).
45. Pang, X. P., Hershsman, J. M., Chung, M. & Pekary, A. E. Characterization of tumor necrosis factor- α receptors in human and rat thyroid cells and regulation of the receptors by thyrotropin. *Endocrinology* **125**, 1783–1788 (1989).
46. Kuleshov, M. V. et al. Enrichr: a comprehensive gene set enrichment analysis web server 2016 update. *Nucleic Acids Res* **44**, W90–W97 (2016).
47. Huang, R. et al. The NCATS BioPlanet - An Integrated Platform for Exploring the Universe of Cellular Signaling Pathways for Toxicology, Systems Biology, and Chemical Genomics. *Front. Pharmacol.* **10**, 445 (2019).
48. Hao, Y. et al. Dictionary learning for integrative, multimodal and scalable single-cell analysis. *Nat. Biotechnol.* **42**, 293–304 (2024).
49. Klatzmann, D. <https://BioRender.com/2pzp78a> (2025).

Acknowledgements

This work benefited from the equipment and services provided by the iGenSeq core facility (Genotyping and Sequencing) and the HISTOMIC platform (Microscopy and Histology) at ICM, Paris. Additionally, this research utilized resources from the CyPS platform (Cytometry) at Pitié Salpêtrière. We extend our gratitude to Nicolas Billiad, Monica Cuevas-Martinez, and Oleg Zubenko for their assistance in various in vitro and in vivo experiments. We also thank Héléne Vantomme and Bruno Gouritin for the cell sortings. We extend our appreciation to Nicolas Coatnan for preparing samples for TCR and single-cell analysis, and to

Kenz Le Gouge for preparing sequencing samples and conducting the initial bulk TCR analysis. We also extend our gratitude to the ViVem Center in Nantes for carrying out the AAV production. Lastly, we thank the UMS28 animal facility, particularly Doriane Joubert-Foret and Flora Issert, for managing the breeding of our mice, Kim Nguyen for monitoring our mice during experiments, and Olivier Br  gerie for supervising the animal facility and providing technical assistance. This work was funded by the TriPoD ERC Advanced Research Grant (FP7-IdEAS-ErC-322856), received by D.K.

Author contributions

J.R. contributed to the experiment design, conducted the in vitro and in vivo experiments, analyzed the corresponding data, and wrote the manuscript. M.F. participated in the majority of the in vivo studies involving murine cells and conducted several experiments. M.D.T. performed the deep phenotyping staining of murine Tregs and some in vivo studies with murine cells in response to the article's peer review. R.F.A. carried out the in vitro experiments for transcriptomic analysis in human Tregs. V.M. analyzed the data from the bulk TCR experiments. M.C. conducted initial in vitro and in vivo experiments at the project's onset. G.F. participated in the euthanasia of mice where organs were collected and processed, and managed all the mouse lines of the laboratory. F.C. scored the histological slides from the autoimmunity induction experiment. N.T. analyzed the transcriptomic data in human Tregs and single-cell transcriptomic data from murine Tregs. T.M. carried out the methylation analysis under B.Y.'s supervision. T.V. and M.R. contributed to project supervision, with T.V. also participating in most of the in vivo experiments and their analyses. D.K. conceived the project, coordinated the work, and wrote the manuscript.

Competing interests

The authors declare the following competing interests: D.K. is the inventor of the patent application related to IL-2-producing Tregs. The remaining authors have no competing interests.

Additional information

Supplementary information The online version contains supplementary material available at <https://doi.org/10.1038/s41467-025-60082-z>.

Correspondence and requests for materials should be addressed to David Klatzmann.

Peer review information *Nature Communications* thanks the anonymous reviewer(s) for their contribution to the peer review of this work. A peer review file is available.

Reprints and permissions information is available at <http://www.nature.com/reprints>

Publisher's note Springer Nature remains neutral with regard to jurisdictional claims in published maps and institutional affiliations.

Open Access This article is licensed under a Creative Commons Attribution-NonCommercial-NoDerivatives 4.0 International License, which permits any non-commercial use, sharing, distribution and reproduction in any medium or format, as long as you give appropriate credit to the original author(s) and the source, provide a link to the Creative Commons licence, and indicate if you modified the licensed material. You do not have permission under this licence to share adapted material derived from this article or parts of it. The images or other third party material in this article are included in the article's Creative Commons licence, unless indicated otherwise in a credit line to the material. If material is not included in the article's Creative Commons licence and your intended use is not permitted by statutory regulation or exceeds the permitted use, you will need to obtain permission directly from the copyright holder. To view a copy of this licence, visit <http://creativecommons.org/licenses/by-nc-nd/4.0/>.

  The Author(s) 2025